ANTIBACTERIAL ACTIVITIES OF SILVER-NANOPARTICLES-TITANIA COMPOSITE THIN FILMS FABRICATED BY THE MOLECULAR PRECURSOR METHOD (MPM)

A RESEARCH THESIS SUBMITTED IN PARTIAL FULFILMENT

OF THE REQUIREMENTS FOR THE DEGREE OF

MASTER OF SCIENCE IN CHEMISTRY

OF

THE UNIVERSITY OF NAMIBIA

BY

MOSES TUHAFENI JOSEPH
(201205728)

April 2019

Main Supervisor: Dr. Daniel Likius (Dept. Chemistry and Biochemistry)

Co-Supervisor: Prof. Marius Hedimbi (School of Medicine)

ABSTRACT

Titanium Oxide (TiO_2) as a photocatalyst produces free radicals upon receiving light energy; thus, it possesses antibacterial properties. The antibacterial property of silver-nanoparticles-doped TiO_2 photocatalysts (Ag-NPs/TiO_2) could be further enhanced by visible light illumination, which also widens its practical applications. However, the major limitation of this Ag-NPs/TiO_2 composite material is its poor miscibility, which subsequently reduces the antibacterial activities of the material. To overcome this limitation, the Molecular Precursor Method (MPM) was adopted in this study as a synthetic method for the fabrication of Ag-NPs/TiO_2 composite thin films with various and unprecedentedly high amounts of Ag-NPs. X-ray Diffraction (XRD) results revealed the presence of metallic Ag and a mixed phase in composite films. For composite films with less Ag content, Field Emission-Scanning Electron Microscopic (FE-SEM) analyses showed well dispensed Ag nanoparticles which appeared uniformly distributed across the films. Particles agglomeration and rough surface morphology were observed in films with high loads of Ag-NPs. Far-reaching absorption across the visible region was observed for composite films and the Surface Plasmon Resonance (SPR) of Ag-NPs is ascribed to the effect. The antibacterial behaviors of resultant films were investigated against a gram negative bacterium, *Escherichia coli* as a model, both in the dark and under visible light by using the Antibacterial Susceptibility Testing method. Composite films were found to have superior bactericidal activity than either neat TiO_2 or Ag-only films, both in the dark and under visible light. Furthermore, films showed enhanced antibacterial activity under visible light than in the dark. In summary, all films exhibited bactericidal effect of different proportions depending on the Ag-NPs content in the titania matrix.

Table of Contents

ABSTRACT ii

LIST OF TABLES v

LIST OF FIGURES vi

CONFERENCE PROCEEDING ix

LIST OF ABBREVIATIONS AND/OR ACRONYMS x

ACKNOWLEDGEMENTS xii

DEDICATION xiii

DECLARATIONS xiv

CHAPTER 1: INTRODUCTION 1

1.1. Background of the study 1

1.2. Statement of the problem 2

1.3. Objectives of the study 2

1.4. Significance of study 3

CHAPTER 2: LITERATURE REVIEW 4

2.1. Overview 4

2.2. Crystal structure and properties of naturally occurring polymorphs of titanium dioxide 6

2.3. Development of visible light active (VLA) TiO_2 photocatalysts 19

2.3.1. Non-metal doping of TiO_2 photocatalysts 19

2.3.2. Noble metal and transition metal doping of TiO_2 photocatalysts 21

2.3.3. Dye sensitization in TiO_2 photocatalysts 24

2.4. Historical background of noble metal nanoparticles 25

2.5. Methods for the synthesis of Ag nanoparticles 28

2.6. Reduction of silver ions to metallic silver 30

2.7. Methods for fabrication of Ag/TiO_2 surfaces 32

2.7.1. Sol-gel method 32

2.7.2. Molecular Precursor Method (MPM) 33

2.8. Mechanism of photo-activity of pure TiO_2, Metal doped-TiO_2 and Nonmetal-doped TiO_2 34
CHAPTER 3: RESEARCH METHODS 36
3.1 Research design 36
3.2. Materials 36
3.3. Procedures 37
3.3.1. Cleaning of quartz glass substrates 37
3.3.2. Preparation of the Titania precursor solution (S_{Ti}) 37
3.3.3. Preparation of the silver precursor solution (S_{Ag}) 38
3.3.4. Preparation of Ag-NPs/ Titania composite precursor solutions and thin films 39
3.3.5. Thin film characterization 41
3.3.6. Antibacterial activity evaluation 43
CHAPTER 4: RESULTS AND DISCUSSIONS 46
4.1. Synthesized precursor solutions 46
4.2. Fabricated thin films 47
4.3. Structural and chemical characterization of thin films 48
4.3.1. Phase analysis 48
4.3.2. SEM analysis 50
4.3.3. Profilometry; thin film thickness analyses 52
4.3.4. Optical property of fabricated thin films 53
4.4. Antibacterial activity evaluation 55
4.4.1. Disk diffusion Method 55
4.4.2. Viable cell count method 58
CHAPTER 5: CONCLUSIONS AND RECOMMENDATIONS 60
a) Conclusions 60
b) Recommendations 61
6. REFERENCES 62
Appendix I: Materials used in this study 80
Appendix II: Data for mean film thickness 82
Appendix III: Raw data for the disk diffusion method 83
Appendix IV; Raw data for the viable cell count method 84

LIST OF TABLES

Table 1: Chemicals used to prepare precursor solutions. 80

Table 2: Consumables used in the antibacterial susceptibility test. 81

Table 3: Mean film thickness for selected films. 82

Table 4: Experimental results for the antibacterial activity evaluation of thin films. 83

Table 5: In the dark 84

Table 6: Under visible light 84

LIST OF FIGURES

Figure 1**:** 'Crystal structures of primary polymorphs of TiO_2, where (a) anatase, (b) rutile and (c) brookite' (12: p.333). 7

Figure 2. 'Variations in the rate of survival of copper-resistant *E. coli* on copper/titania composite thin films' (19: p.8). 10

Figure 3.'Schematic diagram of a photo-electrochemical cell, (1) n-type TiO_2 electrode, (2) platinum black counter electrode, (3) ironically conducting separator, (4) gas burette, (5) load resistance and (6) voltmeter' (27: p.2)..... 11

Figure 4. 'Glass cover on highway tunnel lighting fixtures darkened by automobile exhaust without TiO_2 and maintained clean with TiO_2' (50: p.7). 13

Figure 5. 'AFM images of stearic acid monolayer on TiO_2 film surface before and after UV-light treatment' (19: p.7). 14

Figure 6. 'Photo-induced hydrophilicity and self-cleaning property of a TiO_2-coated surface' (28: p.19)..... 15

Figure 7. 'Conventional tiles under UV light, water forms droplets that dry leaving behind dirt deposits' (28: p.30). 15

Figure 8. 'Photocatalytic tiles under UV light illumination' (28: p.31)..... 16

Figure 9. 'Practical use of the anti-fogging function in vehicle' side mirrors; normal mirror (left) and TiO_2-coated mirror (right)' (19: p.13). 17

Figure 10. 'Photograph of a mouse after initial treatment (A), and 4 weeks after treatment (B)' (21: p.14). Titania powder was inserted into tumour 1. Tumour 2 was never treated with TiO_2. Both tumours were exposed under the same conditions. 19

Figure 11. 'Change in band gap after doping TiO_2 with non-metal (a), UV-Vis absorption profiles of TiO_2 after doped with C and/ or S (b)' (1: p.51). 20

Figure 12. 'Schematic representative diagram of the operation of the TiO_2 band gap after doped with a transition metal (Ni^{2+})' (1: p.54). 22

Figure 13. ‘A plasmonic Z-scheme mechanism of TiO_2/Ag/AgCl composite’ (1: p.56). 23

Figure 14. ‘Schematic of charge transport and interfacial transfer in DSSCs’ (86: p.209). .. 24

Figure 15. ‘Majolica dish. “Pico, Circe e Canente” painted by Xanto Avelli da Urbino and lustred by Mastro Giorgio Andreoli; by courtesy of Museo Civico – Palazzo dei Consoli, Gubbio’ (88: p.517). 26

Figure 16. ‘Flowchart of $citrate^{3-}$ oxidation, silver ion reduction and nucleation of an Ag^{+} precursor by aqueous electrons, respectively’ (1: p.58). 27

Figure 17. ‘Stages of Ag-NPs fabrication’ (1: p.59). 28

Figure 18. ‘Photocatalytic mechanism of bare TiO_2 (hv_1), Ag-doped TiO_2 (hv_2) and non-metal doped TiO_2 (hv_3)’ (68: p.157). 35

Figure 19. Research design flowchart 36

Figure 20. Schematic representation of procedures for the preparation of the titania precursor solution. 38

Figure 21. Schematic representation of procedures for the preparation of the silver precursor solution. 39

Figure 22. 'Fabrication of thin films on quartz glass substrate using the spin coating system' (2: p.107). 40

Figure 23. Photograph of the field emission scanning electron microscopy (FE-SEM) at BIUST. 41

Figure 24. A photograph of a Sloan DEKTA3 profilometer. 42

Figure 25. Photograph of the Perkin-Elmer Lambda 35 UV/Vis spectrophotometer. 43

Figure 26. Antibacterial evaluation procedures of Ag-NPs/TiO_2 thin films (Viable Cell Count Method). 45

Figure 27. Photograph of a 0.4mmol/g TiO_2 (left) and 0.8mmol/g Ag-NPs (right) precursor solutions. 46

Figure 28. Photographs of fabricated thin films with different concentrations of Ag-NPs. .. 48

Figure 29. Wide-angle XRD patterns of the prepared thin films 50

Figure 30. FE-SEM images of (a) 10 mol% Ag, (b) 50 mol% Ag and (c) 90 mol% Ag films. 51

Figure 31. (a) Profilometric scan of a 60 mol% Ag thin film, (b) FE-SEM image of a 60 mol% Ag film. 52

Figure 32. UV–Vis absorption spectra of (a) the a-TiO_2 and Ag-NPs, and (b) composite photocatalyst thin films. 54

Figure 33. Photographs of zones of inhibition test results of selected thin films 57

Figure 34. Mean zones of inhibition of films with different Ag-NPs against the zone of the positive control. Means ± standard errors of 3 replicates are presented. 57

Figure 35. Antibacterial activity evaluation of various thin films in the dark and under visible light. Means ± standard errors of 3 replicates are presented. 59

CONFERENCE PROCEEDING

Moses Tuhafeni Joseph, 2018, Antibacterial activities of silver-nanoparticles/titania composite thin films fabricated by the Molecular Precursor Method (MPM). 6th Annual Science Research Conference, 14 – 15 November 2018, Windhoek, Namibia

LIST OF ABBREVIATIONS AND/OR ACRONYMS

$AgNO_3$	Silver nitrate
Ag-NPs	Silver nanoparticles
Ag-NPs/TiO_2	Silver nanoparticles/titania composite
Bu_2NH	Dibutylamine
CB	Conduction band
CN^-	Cyano radical
CVD	Chemical Vapour deposition
DSSCs	Dye Sensitized Solar Cells
e^-/h^+	Electron-hole pair
e^-	Electron
E. coli	*Escherichia coli*
EDTA	Ethylenediamine-N,N,N',N'-tetraacetic acid
EtOH	Ethanol
eV	Electron volt
FE-SEM	Field emission scanning electron microscopy
HOMO	Highest occupied molecular orbital
LSPR	Localized Surface Plasmon Resonance
LUMO	Lowest occupied molecular orbital
MeOH	Methanol
MPM	Molecular Precursor Method
PVC	Polyvinyl chloride
PVD	Physical Vapour Deposition

ROS	Reactive Oxygen Species
S_{Ag}	Silver precursor solution
$S_{composite}$	Silver: titania composite precursor solution
SPR	Surface Plasmon Resonance
S_{Ti}	Titania precursor solution
TEM	Transmission electron microscopy
TFTC	Too few to count
Ti (O^iPr)$_4$	Titanium isopropoxide
TiO_2	Titania
TMTC	Too many to count
UV	Ultraviolet
VB	Valence band
Vis	Visible light
VLA	Visible light active

ACKNOWLEDGEMENTS

Glory be to the Lord, Jesus Christ for his continual wave of strength upon me, the wisdom and creativity he blessed me with prior, during and after writing this precious piece of work. I would like to extend my heartfelt gratitude to my supervisors and mentors, Dr. Daniel Likius and Prof. Marius Hedimbi for their genuine guidance and mentorship which they have accorded me with throughout my studies. I wish to further extend my sincere gratitude to the federal republic of Germany for having supported my research project by means of placing resources at my disposal, through the German Academic Exchange Services (DAAD). This research work would not have been possible without your financial contribution. Forever, I shall remain indebted to DAAD for their generosity. A great thank you to the Ministry of Mines and Energy, and in particularly to Ms. Martha Amputu for always having allowed me to use their facilities for my research. Equally, I wish to express my profound thankfulness to my close friend, Nande Nghilalulwa, for always fueling me up with words of encouragement since day one of the commencement of this work.

DEDICATION

When the world closed its doors on me, you both opened your arms for me. When people shut their ears for me, you both opened your hearts for me. In light of the foregoing, I hereby wholeheartedly dedicate this work to both of my mothers; mamma Flolian Hamalwa and mama Maria Ekongo. Thank you for always being there for me.

DECLARATIONS

I, **Moses Tuhafeni Joseph**, hereby declare that this study is my own work and is a true reflection of my research, and that this work, or any part thereof has not been submitted for a degree at any other institution.

No part of this thesis may be reproduced, stored in any retrieval system, or transmitted in any form, or by means (e.g. electronic, mechanical, photocopying, recording or otherwise) without the prior permission of the author, or The University of Namibia in that behalf.

I, Moses Tuhafeni Joseph, grant The University of Namibia the right to reproduce this thesis in whole or in part, in any manner or format, which The University of Namibia may deem fit.

…….. ……. …….

Name of student Signature Date

CHAPTER 1: INTRODUCTION

1.1. Background of the study

Titanium dioxide has (TiO_2) increasingly attracted considerable attention in research due to its excellent photocatalytic property (1) and subsequent photo-induced antibacterial activity (2–4). TiO_2 is one of the few most effective photocatalysts that is presently in use because of its strong oxidizing ability, stability, low cost and non-toxicity property (4). When TiO_2 is illuminated with UV light, it exhibits robust antibacterial activity (5). The photo-generated holes (h^+) and electrons (e^-) react with atmospheric water and oxygen, respectively, to yield some reactive oxygen species (ROS) such as superoxide anions (O_2^-), hydrogen peroxide (H_2O_2) and hydroxyl radicals (·OH) (6), which are strong and unselective oxidizing agents for the degradation of a wide range of organic matters including bacteria. Thus, TiO_2-incorporated materials are able to kill bacteria under UV irradiation. Neat TiO_2 has been extensively reported to only absorb in the UV region (3,7–11). However, UV light accounts for only 4 – 6% of the total solar energy, which is inadequate for photocatalysis (low quantum yield) (1). While the solar spectrum constitutes about 40% of visible light (12).

In an effort to maximally harness as much energy of the solar spectrum as possible, numerous efforts have been invested on research in shifting the excitation wavelength of TiO_2 into the visible region (13). This does not only result in enhanced photocatalytic activity of the material but it also improves the inherent photo-induced bacterial killing ability of the material (14). One of the approaches for achieving this, is by introducing foreign species such as: noble metal nanoparticles into the titania matrix (1,15,16). In this study, titania was doped with Ag nanoparticles, and thin films

of the resultant composite solution were prepared on quartz glass substrates. Their optical property and subsequent antibacterial activity were investigated.

1.2. Statement of the problem

Antibacterial activity of Ag/TiO_2 composite films fabricated by the Molecular Precursor Method (MPM) has not been reported in the literature yet, though the bactericidal effect of Ag/TiO_2 composite films prepared using different synthetic methods other than the MPM has been widely reported (2-9). Although Ag/TiO_2 thin films containing up to 80 molar % of Ag nanoparticles suspended in TiO_2 matrixes were successfully fabricated using the MPM in previous studies (1,17), their antibacterial properties have not yet been reported. Therefore, in this research, silver-nanoparticles/titania (Ag-NPs/TiO_2) composite thin films were synthesized and their antibacterial activities were investigated against *Escherichia coli* as a model for gram-negative bacteria.

1.3. Objectives of the study

(a) To fabricate Ag-NP/TiO_2 composite thin films with different Ag-NPs molar concentrations using the MPM.

(b) To study the surface morphology, chemical compositions, film thickness and optical properties of the fabricated thin films.

(c) To investigate and compare the antibacterial activities of the fabricated thin films on *E. coli*.

1.4. Significance of study

This study, for the first time, provides information on unexplored antibacterial activity of Ag-NPs/TiO_2 composite thin films fabricated by the MPM which has also laid a foundation for understanding the antibacterial activities of Ag-NPs/TiO_2 films synthesized using the MPM.

CHAPTER 2: LITERATURE REVIEW

2.1. Overview

Nanotechnology involves the study and manipulation of extremely small objects of size ≤ 100 nm that could be used as building blocks for a material whose bulk properties are different from the properties of each of its component (1,2). There are currently high hopes amongst experts in the field of material science that the discipline of nanotechnology has the potential to lead to the development of new compounds that could be utilized towards the betterment of people's lives. As a result, researchers have been working on developing both nanostructured inorganic and organic antibacterial agents. Although, both inorganic and organic antibacterial materials have been used in the past for disinfection applications (10), scientists are more attracted to work with inorganic compounds because of the vast benefits they offer over the organic compounds (7).

Silver (Ag) is one of the inorganic elements that have long been accepted as an effective antibacterial agent owing to its low toxicity-property in living cells and it is known to show diverse in vitro and in vivo applications (8). In fact, literature has it that Ag has been used during the ancient times for prevention of infections, handling and cleaning of burns, catheter, trauma and dental amalgam for thousands of years (4,13). Previous studies have shown that both silver ions and silver nanoparticles (Ag-NPS) exhibit antibacterial activity (2,4,11,18–20). Titanium dioxide (TiO_2) also called titanium (IV) oxide or titania has increasingly attracted attention in research due to its excellent photocatalytic (1,11,13,14,20–25) and photo-induced antibacterial activity (15,26).

Titania is one of the few most effective photocatalysts that is presently in use because of its strong oxidizing ability, stability, low cost and non-toxicity property (7). Substantial research on TiO_2 semiconductors is currently underway because of the wide range of possible applications linked with the material. Research by Fujishima and Honda (27) has shown how TiO_2 as a semiconductor could split water into hydrogen (H_2) and oxygen (O_2) in a photo-electrochemical cell (5,27–29). Furthermore, their work triggered a scientific research revolution on semiconductors, which in the year 1977 led to Frank and Bard having further demonstrated the unique properties of titanium dioxide for environmental remediation through the reduction of Cyano (CN^-) in water (30). In a different study by Alfonso, 1998 (31), it was demonstrated how TiO_2 photocatalyst was used in the purification of polluted water. After O'Regan and Gratzel's paper on the Dye Sensitized Solar Cells (DSSCs) was published in the 1990's (32), titania emerged as one of the most researched semiconductor materials in the world, as evidenced by the escalation in the number of publications since then.

Although many past studies on titania had focused on the material's responsiveness to UV-light, the study of titania with respect to visible-light-responsiveness and the incorporation of Ag-NPs in the titania matrix has gained momentum in recent years; as it has shown potential industrial applications in not only solar energy production (21,22,29), decontamination (2,4,7,11,13–15,18,19,23,25), but also in the development of self-cleaning materials (5,18,33) and antifogging materials (5,21,28).

Titania is n-type semiconductor with a proven wide band gab which enables it to respond only to ultraviolet light (photon of light < 400 nm), thereby limiting its practical applications under the visible light region (400 nm-700 nm) (34). Therefore, in order to exploit TiO_2 to its full potential, it is essential to reduce the band gab size by doping it with impurities such as, silver (Ag) (2), nitrogen (N) (15,35,36), carbon (C) (37,38), sulfur (S) (16) and by incorporating dye into the titania matrix to facilitate visible light absorption. Although a number of studies have been carried out on TiO_2 doped with components mentioned herein above under UV light illumination, the solar spectrum only consists of about 4-6% of UV-light, which is not adequate for efficient photocatalysis (2). Thus, one of the objectives of this study was to develop visible-light-responsive antibacterial Ag-NPs/TiO_2 photocatalysts by shifting the threshold of the photo-response of titanium dioxide into the visible light region through doping TiO_2 with Ag nanoparticles.

2.2. Crystal structure and properties of naturally occurring polymorphs of titanium dioxide

TiO_2 exists in three main phases: anatase, rutile, of which each assumes a tetragonal crystal system, and brookite, which appears orthorhombic (21). The structures of these phases can be understood in terms of (TiO_2^{6-}) octahedral. The three crystal structures differ by the distortion and linkage of the octahedral chains. Anatase can be regarded to be built-up from octahedral that are connected by their vertices, in rutile, the edges are connected, and in brookite, both vertices and edges are joined (21,39). Experimental data indicate that rutile is the most stable phase at all temperatures and pressures, followed by the anatase phase and ultimately the brookite phase (40) .

Figure 1 shows the crystalline structures of the three main polymorphs of titania as cited by Pelaez *et al*. (22).

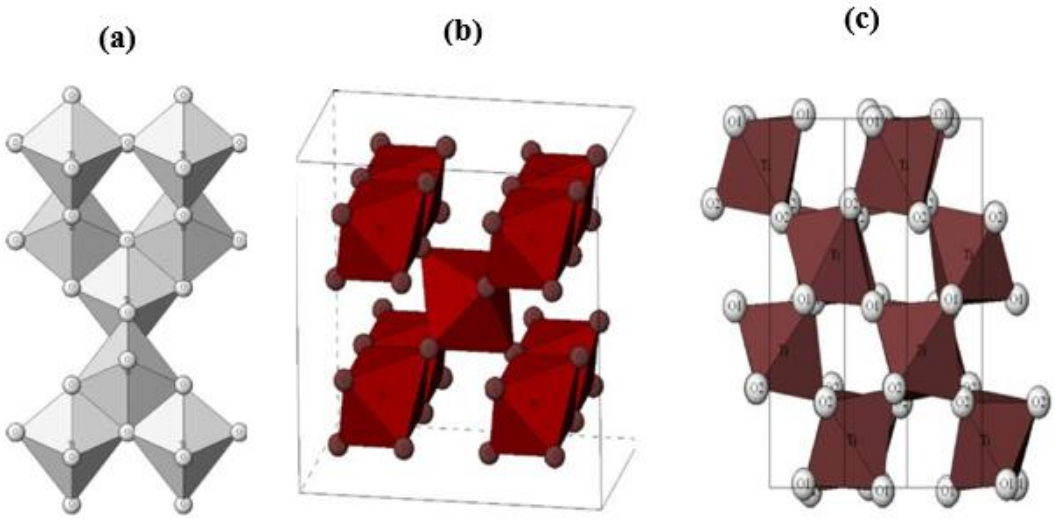

Figure 1: 'Crystal structures of primary polymorphs of TiO_2, where (a) anatase, (b) rutile and (c) brookite' (12: p.333).

The chemical and physical properties of TiO_2 such as; high stability, non-toxicity and low-cost make it an attractive photocatalyst (41). Titanium dioxide does not absorb visible light, thus, it has a white color (19). It is this property that makes it possible for titania powders to be used as white pigments during the olden times (19,20). TiO_2 is chemically stable only in the dark, it however, absorbs in the ultraviolet region (< 400 nm) which induces some chemical reactions (8). Such activity (reactions) can be justified from observations made during the ancient times. Among them was the peeling of paints from the walls, and the dilapidation of fabrics integrated with titania upon continuous exposure to UV-light (42)

There have been studies reported on photo-reactivity of titania as of the early 20th century. For instance, in 1938, there was a paper by Doodeve and Kitchener on the

utilization of TiO_2 for photo-bleaching of dyes both in vacua and in the presence of oxygen as cited by Hashimoto *et al*. (19). As conveyed in the report, it was observed that active oxygen species including; superoxide anion (O_2^-) and hydroxyl radical ($\cdot OH$) are produced on the surface of titania upon UV illumination (28,43), which subsequently result in the photo-bleaching of dyes. It is also worth noting that the authors of this paper under discussion were certain that there was no alteration in TiO_2 throughout the photoreaction in spite of them having used the terminology photosensitizer in their article instead of the term "photocatalyst", stated Hashimoto *et al*. (28).

In Japan, the utilization of the photochemical power of TiO_2 to induce chemical reactions actively has long been realized. In 1956, there were sequences of reports by Serpone *et al*.(43), in particular, a paper titled "Auto-oxidation by TiO_2 powders into different organic solvents", which they exposed to UV irradiation by using mercury (Hg) lamp. Auto-oxidation of solvents and formation of hydrogen peroxide (H_2O_2) under ambient conditions were observed. Their report indicates that after a series of experiments they observed that the titania powder in the form of anatase exhibited relatively high auto-oxidation activity than the titania powder in rutile form. However, during that era the photocatalytic power of TiO_2 might not had attracted the full attention of scientists and, hence, there was no significant development of TiO_2 photocatalysis reported at that time, both in academic and industrial society.

The photo-induced bactericidal and detoxification effects of titania was first reported by Matsunaga *et al*. as cited by Akhavan and Ghaderi (9). Titanium dioxide photocatalysis can be used to kill and remove bacteria, for this reason, self-sterilizing surfaces such as; thin films can be prepared. The UV illumination of intensity,

1mW/cm^2 on the TiO_2 surface could absolutely bring about the disappearance of *E. coli* cells from the surface in about 7 days. The complete killing and removal of bacterial cells can be realized in a very short irradiation time, depending on the intensity of the incident rays (44). The intensity of a usual indoor UV light is, however, way too weak than the outdoor one. Thus; the photo-killing of bacterial cells under indoor settings would take much longer than under outdoor conditions.

The doping of TiO_2 photocatalysts with noble metals improves not only the photocatalytic property but also the antibacterial killing function of the materials even under weak UV light exposure from a fluorescent light bulb. Figure 2 indicates levels of survival of copper resistant *E. coli* cells inoculated on a Cu/TiO_2 composite thin film. Results from this figure show that after several hours of incubation in the dark, only a very small and negligible number of *E. coli* cells were eliminated from the film. On the other hand, the rate of survival of cells begun to drop significantly with increase in the duration of illumination when the film was irradiated with weak, yet enough UV light. This reveals the photo-induced antibacterial activity of TiO_2/metal-doped surfaces under weak UV irradiation supplied by a fluorescent lamp in an indoor setting as cited by Guo *et al*. (45).

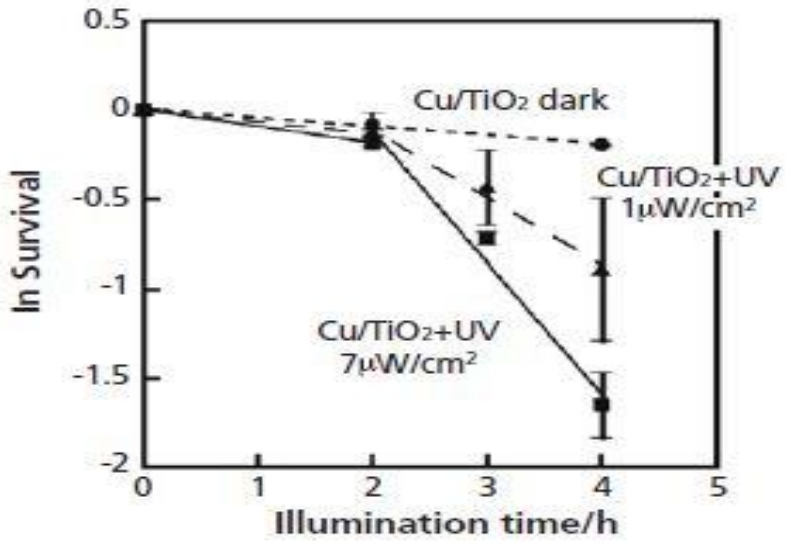

Figure 2. 'Variations in the rate of survival of copper-resistant *E. coli* on copper/titania composite thin films' (19: p.8).

Similar work was reported in the year 1997 and 1998 (46,47). The self-sterilizing effect of TiO_2 was demonstrated in a case of food poisoning from *E. coli* in western Japan in 1996. It was reported that there was a severe outbreak, in which nearly 2000 people were hospitalized and 12 fatalities recorded. It was found that the poisoning was caused by the *O-157* endotoxin of *E. coli*. In an attempt to mitigate the outbreak, Kikuchi *et al.* (46) employed TiO_2 photocatalysis examination as a mean of decomposing this lethal toxin. It was noted that the material (TiO_2) was able to deactivate and remove the toxin. Moreover, their method is comparable to the rest of the techniques that have been developed for this purpose (47).

Although, the photo activity of titania was reported as far back as the 20th century, studies on the investigation of the photo-activity of TiO_2 incorporated materials for various purposes only began picking up rapidly after a breakthrough research by Honda and Fujishima (27) was published in *Nature* in 1972. Hydrogen (H_2) is considered as an ideal fuel for the future. Thus, in an effort to work towards solving

the issue of energy-shortage in the world, the duo started investigating the photocatalysis of water in 1969 by using a single crystal n-type TiO_2, rutile semiconductor electrode and a platinum black counter electrode to split water into H_2 and O_2. The driving force behind their research was the scarcity of crude oil in those days, which resulted in the sky-rocketing of oil prices. Hence, according to Hashimoto *et al*. (28), this period became known as the 'time of oil crisis'. Given the situation, their report managed to attract the attention not only of electrochemists but also of many other researchers in related areas. Thereafter, a number of related papers were widely reported (28). Below is figure 3, which demonstrates the Honda-Fujishima effect.

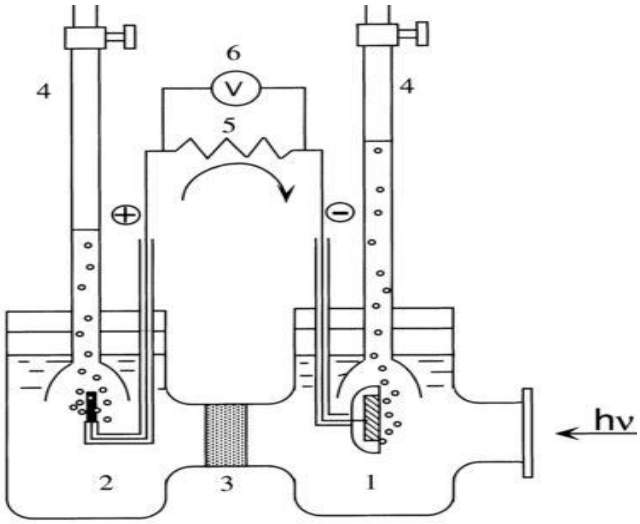

Figure 3.'Schematic diagram of a photo-electrochemical cell, (1) n-type TiO_2 electrode, (2) platinum black counter electrode, (3) ironically conducting separator, (4) gas burette, (5) load resistance and (6) voltmeter' (27: p.2).

One of the nano-functions that have widely been explored in the construction industry is undoubtedly the photocatalytic self-cleaning effect, with Japan taking the lead in this industry (28). There are a number of buildings of different sizes in many mega cities around the world that employ this function. The major effect that this has is that;

it significantly reduces the degree of dirt adhesion on surfaces as opposed to the common assumption that; a surface needs not be cleaned at all.

It is important to note, that the self-cleaning effect only helps to considerably extend the intervals between cleaning cycles which implies that fewer detergents are needed. This yields less negative impacts on the environment, and also cuts on consumables' cost. All in all, photo-induced self-cleaning requires low maintenance and it is a trouble-free solution. For the photocatalytic self-cleaning to be realized, UV light, oxygen and air humidity are required. The amount of UV light that is present in normal daylight alone is enough to bring about a photocatalytic reaction. Following UV illumination, the organic dirt on the surface of TiO_2 begins to decompose with the help of anatase TiO_2, as a catalyst.

The photo-induced self-cleaning effect of TiO_2-coated materials was first reported in 1992 by Hashimoto *et al.* (28). Two years later, the Japanese tiles producer, Toto Ltd, in collaboration with the research team of the University of Tokyo developed and launched photocatalytic tiles on the market. Today, these tiles are widely marketed not only in Japan, but also in other different countries by licensed distributors. After the successful manufacturing of the self-cleaning tiles, many other commercial products were developed using this effect, such as; the self-cleaning cover-glass for tunnel lights, and window blinds Hashimoto *et al.* (28). A typical application of the light-cleaning example is the use of sodium lamps in most tunnels as sources of light in Japan.

There, however, had been a concern with the constant reduction of light intensity in tunnels, resulting in dark and consequently poor visibility in tunnels. The situation had forced researchers to investigate the issue and after close examination, it was found that the decrease in light intensity was due to vehicles 'exhaust fumes that form films on the cover-glass of tunnel lights. During these investigations, it was noted that the high pressure sodium light bulbs also emit UV light at a position of its cover-glass. The released UV light is adequate to prompt complete photo-degradation of these exhaust compounds without the aid of any external UV light sources in order to keep the cover-glass clean when it is coated with TiO_2 photocatalysts (45). Figure 4 below demonstrates the self-cleaning property of TiO_2-coated glass tunnel covers.

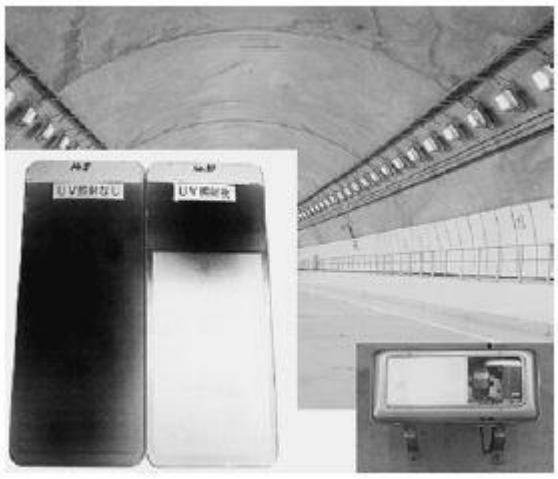

Figure 4. 'Glass cover on highway tunnel lighting fixtures darkened by automobile exhaust without TiO_2 and maintained clean with TiO_2' (50: p.7).

Another scenario that demonstrates the photo-decomposition effect of organic pollutants on TiO_2 surface is one reported by Minabe and his team (48) and by Zaleska (49). Here, a highly packed stearic acid prepared on a titania rutile single crystal was exposed to UV light at an interval of 5 minutes for 20 minutes. It was observed that there had been an increasingly formation of indentations in the surface of the film. And

with further UV irradiation, the pits merged thereby forming a mosaic which eventually vanished as the reaction proceeded. This suggests the complete decomposition of stearic acid by TiO_2 to carbon dioxide. Figure 5 below shows morphological changes in the structure of the film under UV illumination over a period of time.

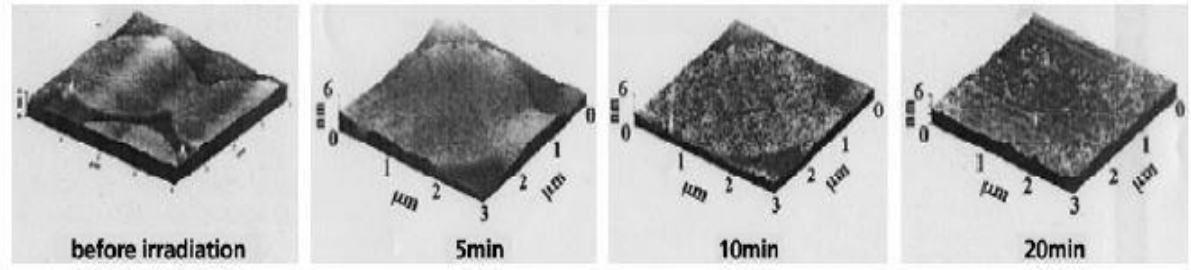

Figure 5. 'AFM images of stearic acid monolayer on TiO_2 film surface before and after UV-light treatment' (19: p.7).

Another interesting and worth discussing property of TiO_2-coated surfaces is the photo-induced hydrophilicity. This property was accidently discovered by Hashimoto *et al.* (28) in 1995 when they were studying the unique concept of light-cleaning TiO_2-coated materials under weak UV illumination in 1990s. Since then, the application range of TiO_2 coatings has expanded greatly, from exterior tiles to façade glass, tents, aluminum walls and PVC fabric. According to Hashimoto *et al.* (28), "the surface wettability is assessed by measuring the water contact angle (CA) which is described as the angle between the solid surface and the tangent line of the liquid phase at the interface of the solid-liquid-gas phase".

When a TiO_2-coated surface is irradiated with UV light such as the one present in Sunlight, organic dirt and grime is broken down and decomposed. Moreover, the material becomes hydrophilic (water-attracting) due to its increased surface energy,

and when exposed to; for example rainwater, it spreads to form a film on TiO_2 surface rather than droplets. Thereby washing away loose dirt and results in a clean surface as depicted in figure 6 below.

Figure 6. 'Photo-induced hydrophilicity and self-cleaning property of a TiO_2-coated surface' (28: p.19).

Specific and practical examples of the photo-induced hydrophilicity of surfaces coated with TiO_2 is the development of photocatalytic building materials such as; exterior tiles (figure 6 and 7), glass, aluminum walls, and PVC fabric. In 2005 the first photocatalytic glass was installed in the terminal building of Chubu international Airport in Japan (28).

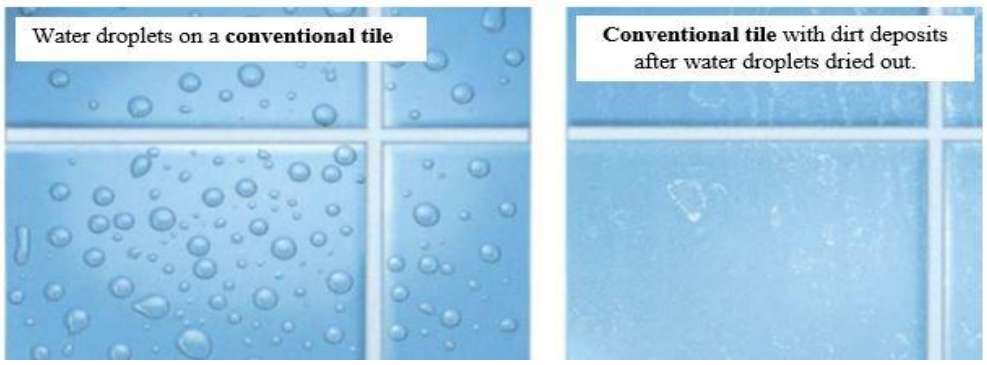

Figure 7. 'Conventional tiles under UV light, water forms droplets that dry leaving behind dirt deposits' (28: p.30).

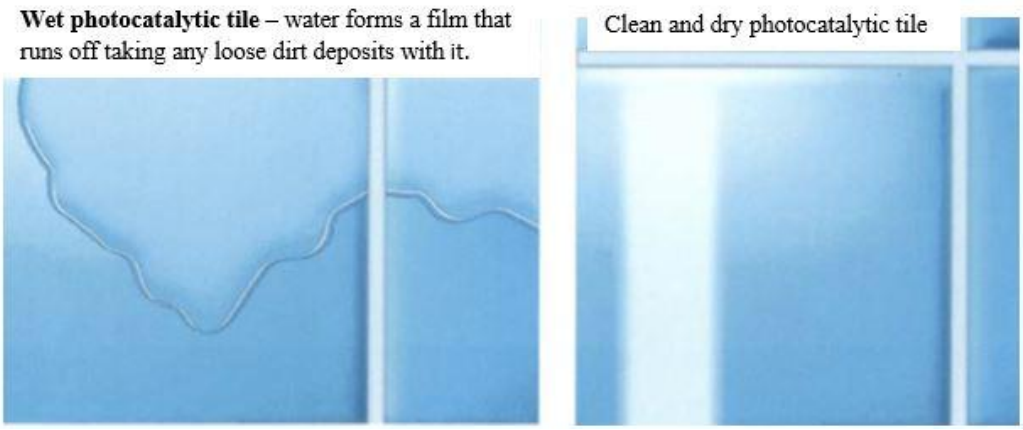

Figure 8. 'Photocatalytic tiles under UV light illumination' (28: p.31).

In addition to the photocatalytic self-cleaning property of TiO_2, there exists another function associated with the photo-induced hydrophilicity property of the material. This function is the 'anti-fogging' ability of the TiO_2-coated surfaces. Hashimoto *et al.* (28) claim that fog takes place on mirror and glass surfaces when water vapors on these surfaces condense to give rise to numerous water droplets. He argues that fog does not form on a highly hydrophilic surface such as that of TiO_2, instead, an even thin film of water forms thereby inhibiting the formation of fog. After the surface becomes highly hydrophilic, it remains as such for a long period of time. As a result, the anti-fogging function could be integrated into different glass products, i.e. from automobile side-view mirrors to façade glasses. This technology has already been adopted by the Japanese automobile manufacturing companies as illustrated in figure 9.

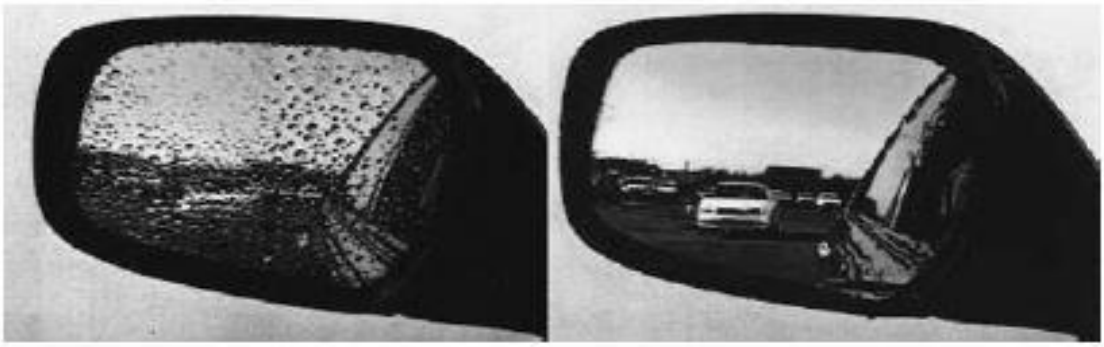

Figure 9. 'Practical use of the anti-fogging function in vehicle' side mirrors; normal mirror (left) and TiO_2-coated mirror (right)' (19: p.13).

Scientific reports on photocatalytic cancer treatments were reported as far back as the mid-1980s. During that time, researchers tried taking advantage of the strong oxidizing power of illuminated TiO_2 to kill cancer cells. A study by Fujishima *et al*. (5) demonstrates how a polarized, irradiated titania film electrode, as well as an illuminated titania colloidal suspension was used in the effective killing of HeLa cell lines. After this research, a series of other related studies subjected to different conditions followed (50–52), including the study in which according to Cai *et al*. (51), the effect of superoxide dismutase was examined and it was found to enhance the photo-killing of cancer cells, due to the production of peroxide.

Furthermore, Cai *et al*. (51) noted that the selective killing of a single tumor cell is possible by utilizing a polarized, illuminated titania microelectrode. In another experiment carried out in 1992, cancer cells were introduced into a mouse to induce tumors to form. Following the formation of tumors, a fine-particle solution of TiO_2 was injected into a mouse, subsequently; the affected parts of the mice were exposed to irradiation. It was observed that the treatment successfully inhibited the growth of tumors. Although, this technique was able to impede the growth of tumor cells, it

however, was not effective in stopping a cancer that had developed beyond stage 1 (54). Therefore, in an effort to resolve this issue, a device was developed which enables the cancer cells to be exposed to illumination while adding titanium dioxide powder to the tumor. It was noted that this device required further refinement before it could be brought into practical use (48). The medical applications of TiO_2 in the past decades do not only demonstrate how relevant this material is in the discipline of medicine, but also reveal the need for further research in the field of photochemistry and catalysis. Figure 10 shows the photograph of a mouse test of a photocatalytic cancer therapy.

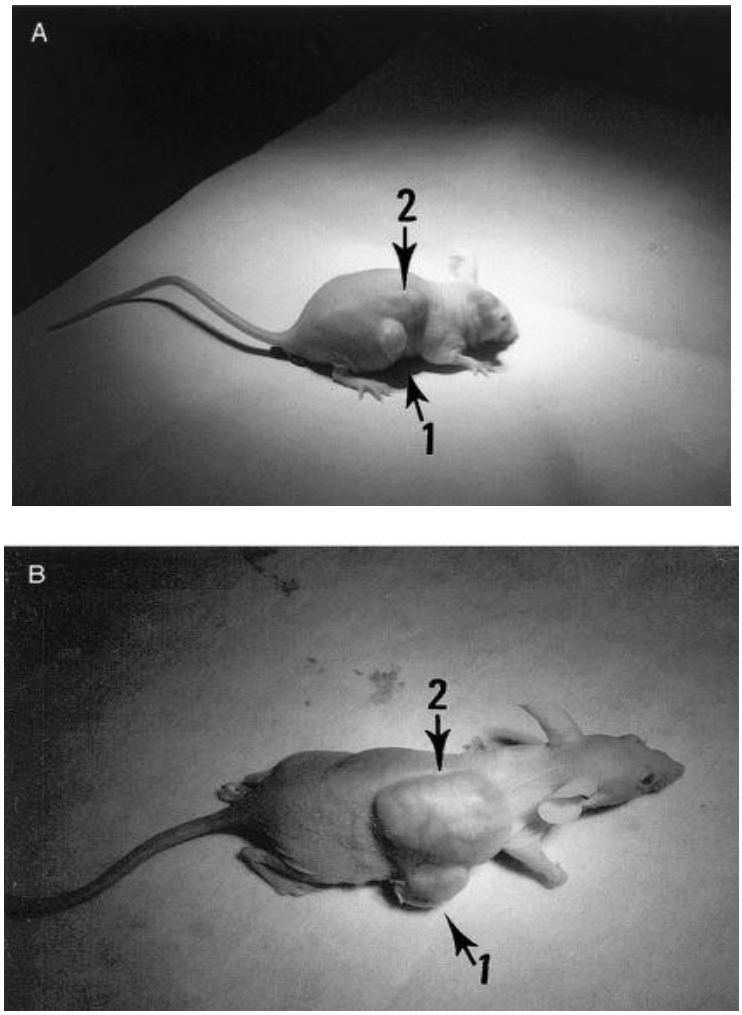

Figure 10. 'Photograph of a mouse after initial treatment (A), and 4 weeks after treatment (B)' (21: p.14). Titania powder was inserted into tumour 1. Tumour 2 was never treated with TiO_2. Both tumours were exposed under the same conditions.

2.3. Development of visible light active (VLA) TiO_2 photocatalysts

2.3.1. Non-metal doping of TiO_2 photocatalysts

Ever since Sato demonstrated the incorporation of nitrogen into the titania matrix in 1986, which resulted in a visible-light-responsive material (53,54), there has been an increase of scientific reports on non-metal doped-TiO_2 photocatalysts such as; carbon doped TiO_2 (37,38), sulfur doped-TiO_2 (16), and fluorinated co-doped-TiO_2 (55,56). Nitrogen has an atomic size that is comparable to that of oxygen, it also has low energy

of ionization, and lastly it is highly stable. These properties enable nitrogen to be easily integrated into the TiO_2 structure (57), as initially established by Sato (53), and reaffirmed by Asahi *et al.*(58). They claimed that the introduction of nitride ions at the oxygen site of titania reduces the band gap, thus, allowing it to absorb in the visible region. Therefore, the nitrogen-substitutable doping has been adopted as a method to narrow the band gap of photocatalysts by altering the valence band structure. Nowadays, impurities such as; C, S, and F are also used as dopants to shift the energy levels above the TiO_2 parent valence band, consequently, allowing thin films to be active to visible light (49), as illustrated in figure 11 bellow by Hamal *et al.* as cited by Daniel *et al.* (1).

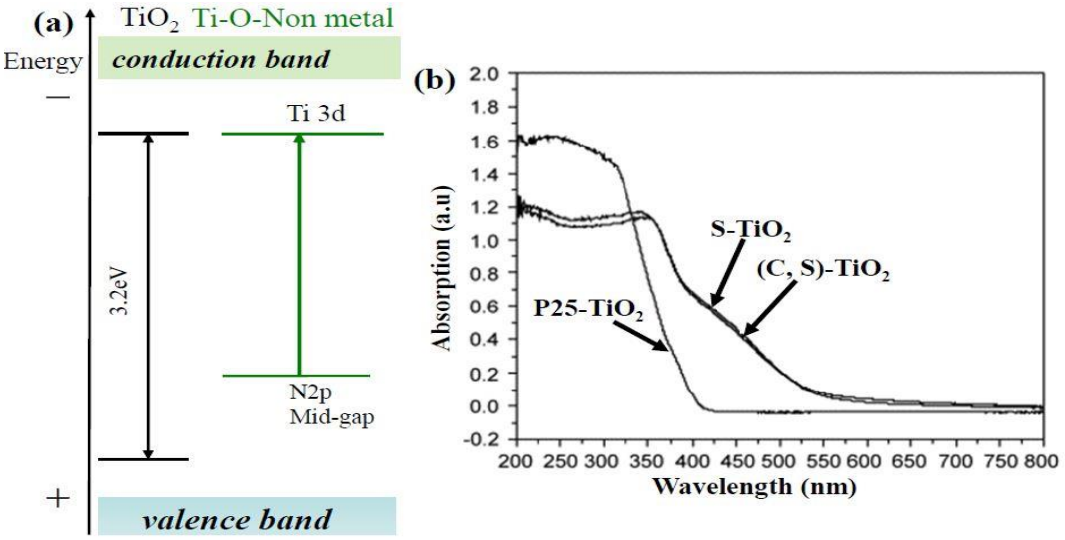

Figure 11. 'Change in band gap after doping TiO_2 with non-metal (a), UV-Vis absorption profiles of TiO_2 after doped with C and/ or S (b)' (1: p.51).

Although studies by Sato (53) and Asahi *et al*. (58) have claimed that the presence of nitrogen in the TiO_2 matrix is the one that reduces the band gap, which subsequently results in the visible-light-responsiveness ability of the material, Ihara *et al.* (59) proposed, that it is the creation of oxygen vacancies that brings about the sensitivity in the material to respond to visible light instead, and that the nitrogen only increases the stability of the oxygen vacancies. Furthermore, the role of oxygen vacancies in enabling visible light sensitivity was also observed in plasma-treated TiO_2 photocatalysts (1). The same effect of oxygen vacancies on visible light responsiveness was for the third time confirmed by Irie *et al*. (60) in a separate study. According to Daniel *et al*. (1), there is currently an agreement on the mechanism of nitrogen doped photocatalysis as outlined by Nagai *et al*. (61).

2.3.2. Noble metal and transition metal doping of TiO_2 photocatalysts

Another way of facilitating visible light-absorption ability of Titania semiconductors is to introduce transition metals or noble metals into TiO_2 framework. The incorporation of transition and noble metals in TiO_2 systems has been proven to not only enhance the photo activities of the emergent material but also increases the antibacterial activity (11,62). However, it is noted that doping with transition metals may also result in reduced quantum efficiency because they could serve as electron/hole (e^-/ h^+) recombination sites.

Furthermore, the thermal instability observed in transition metal-doped TiO_2 materials is attributed to the presence of these metals (63). As reported by Kang (64), the photocatalytic activity of transition metal-doped titania semiconductors has not

significantly improved although a decline in the band gap energy has been reported by many researchers. He suggested that, it is due to the fact that transition metals are not incorporated into the TiO_2 matrix but rather are adsorbed on the surface of titanium dioxide, which shields reaction sites on TiO_2 (64). Transition metals such as; Cu, Fe, Co, Ni, Mn, Nb, W and Ru have been reported to have been used in the modification of TiO_2 photocatalysts (65–70). As a result of doping with transition metals, new energy levels may form between the VB and the CB as demonstrated in figure 12 below, thereby triggering a shift in the excitation wavelength of TiO_2 towards the visible light region. Photo activities depend on the concentration nature of the metal dopant.

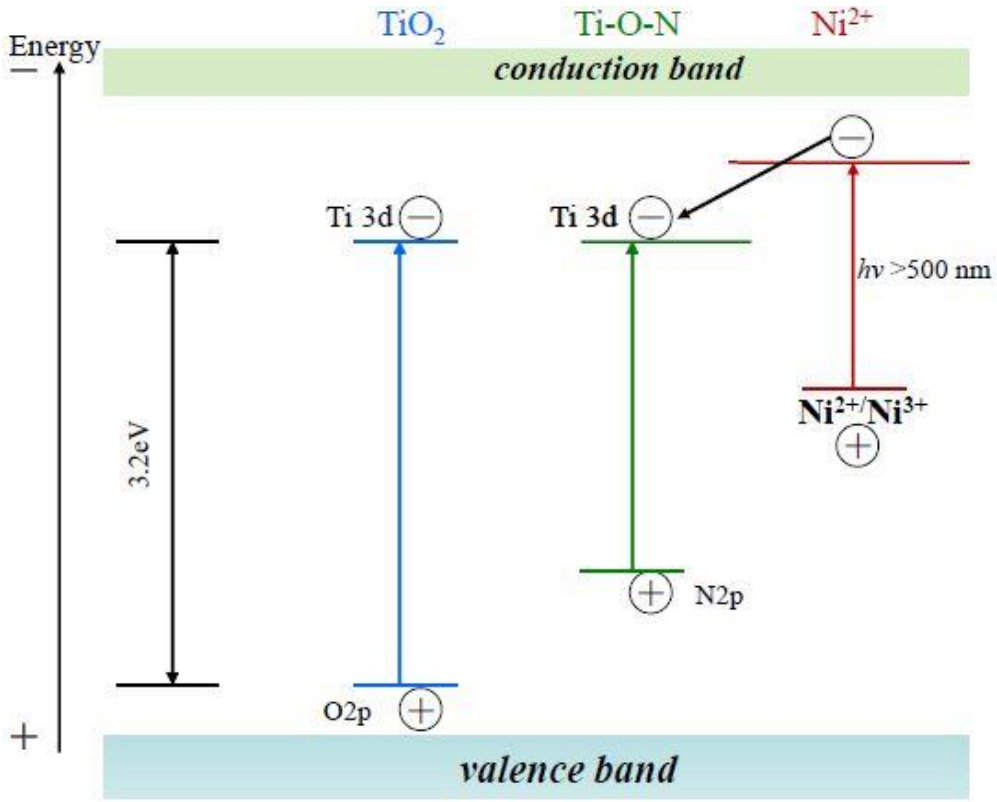

Figure 12. 'Schematic representative diagram of the operation of the TiO_2 band gap after doped with a transition metal (Ni^{2+})' (1: p.54).

The integration of noble metals, namely; Ag, Pt, Pd and Au in the titania system increases the photonic efficiency under visible light by serving as acceptor centers that trap photo-generated e^- and also by promoting interfacial charge transfer, thereby hindering e^-/h^+ pair recombination (71–74). Various studies have been reported in support with statements made herein above, such as that of Sharma (75) *et al*. in which he indicated that deposits of platinum on the surface of titania trap photo-generated electrons, and consequently enhance the photo-induced electron transfer rate at the interface. Seery *et al*. (76) and Daniel *et al*. (1) in separate studies have reported on how Ag-NPs in TiO_2 contributed to the enhancement of the photo activities of the photocatalyst under visible light. It was reported that the improved visible light responsiveness of titania is ascribed to the Surface Plasmon Resonance (SPR) of Ag-NPs (1,77) as shown in figure 13 below.

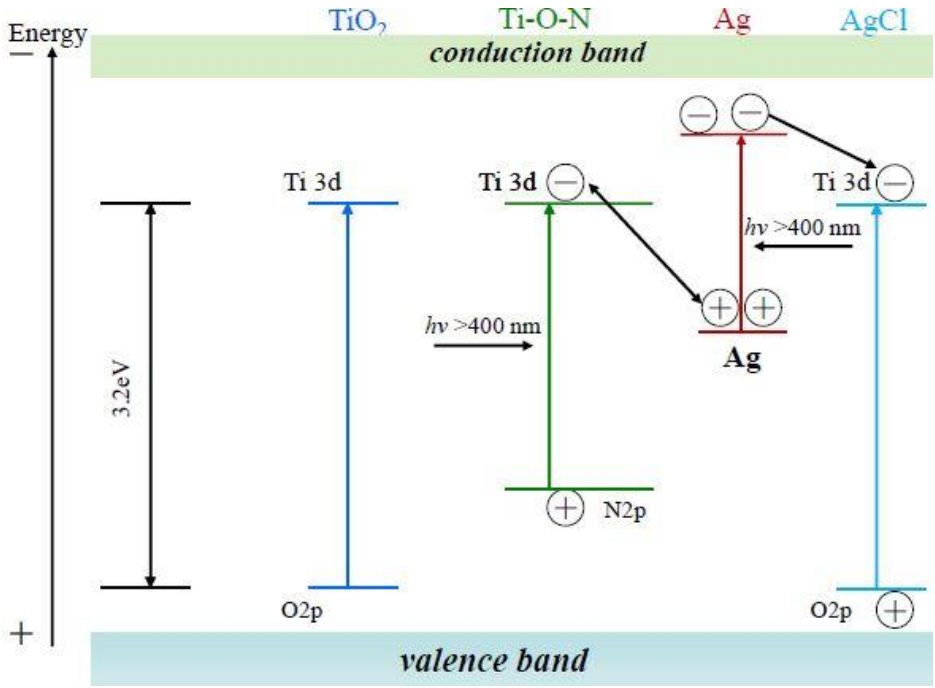

Figure 13. 'A plasmonic Z-scheme mechanism of TiO_2/Ag/AgCl composite' (1: p.56).

2.3.3. Dye sensitization in TiO_2 photocatalysts

The incorporation of various dye sensitizers such as; Ruthenium-based dyes, catechol, phythalocyanines, porphyrins etc. in TiO_2 systems have widely been explored and regarded as one of the methods of shifting the titania photo-responsive ability towards the visible light region (78–80) . A typical application of the dye sensitizers in photocatalysis is the well-known 'Gratzel solar cell (1991) or simply Dye Sensitized Solar Cells (32) as illustrated in figure 14 below. In systems with sensitizer, a dye absorbs visible light, consequently an e^- is excited from the highest occupied molecular orbital (HOMO) to the lowest occupied molecular orbital (LUMO) of the dye. The excited dye then injects electron into the TiO_2 semiconductor. The injected electrons are then rapidly transferred to the surface of the TiO_2, where they are hunted by reactive oxygen species for further reactions (81,82). Although different dye sensitizers have been explored for this purpose, most of them are poisonous. In addition, they may degrade themselves, leading to limitations in their usefulness for the purpose of long-lasting applications in photocatalysis (2).

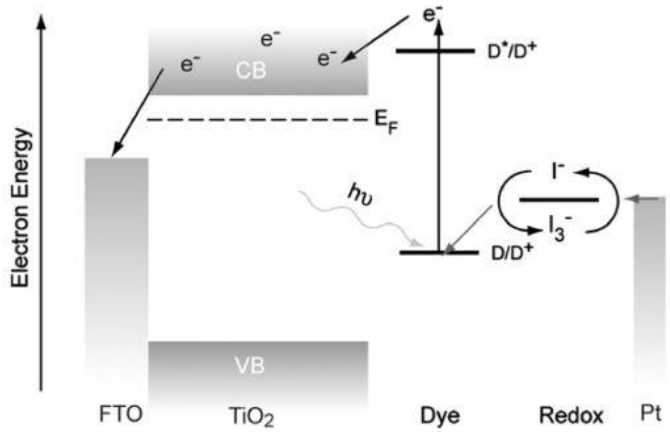

Figure 14. 'Schematic of charge transport and interfacial transfer in DSSCs' (86: p.209).

2.4. Historical background of noble metal nanoparticles

An ancient documentation indicates that solutions of colloidal gold, silver and lead oxides were used for decoration of pottery during the Renaissance period (83). For instance, in Italy, a lustre technique which was first invented in Iraq during the 9th century (84), was adopted in Italian peninsula by local potters as a mean for coating their pottery with a thin metallic film containing silver, copper and other substances (85), this coating gives their pottery beautiful iridescent reflections of various colors, particularly, an intense golden-yellow and ruby-red color. The pottery-coloring process, specifically the glass-coloring refinement was advanced by Andreas Cassius and Johann Kunchel in the 17th century. The duo, contrived a precipitate of colloidal gold and stannic hydroxide (purple of Cassius) into a base glass (85). It is significant to point out that lustre, gold-ruby glasses, Lycurgus cup, and Maya blue are some of the most ancient nanophase materials produced in the past (84,86).

Although, the lustre technique originated from Arabic countries, the Italian artisans, i.e. the likes of Mastro Giorgio Andreoli da Gubbio (87,88) managed to build fame in the pottery industry across Europe in the 15th century, because of his unique initiative of optimizing the traditional lustre technique to yield much better results, which were impossible to reproduce during his time. Today, his optimization recipe of the lustre technique remains a mystery (84). As a result, many other potters used to send their crafts to Giorgio for final touches. A typical example is of a most ancient nanophase lustred material is the Majolica dish by Xanto Avalli da Urbino and Mastro Giorgio, as shown in figure 15 below. Furthermore, Au and Ag nanoparticle solutions have been used in medicine during the Middle Ages because they were believed to possess curative powers for various diseases such as, venereal and heart problems, dysentery,

epilepsy, tumors and also for diagnosis of syphilis. A procedure that had been employed until the 20th century although, it is not completely reliable (85).

Figure 15. 'Majolica dish. "Pico, Circe e Canente" painted by Xanto Avelli da Urbino and lustred by Mastro Giorgio Andreoli; by courtesy of Museo Civico – Palazzo dei Consoli, Gubbio' (88: p.517).

Nonetheless, it is the work of Michael Faraday in the 1850s that marked the first ever reported scientific study on metal nanoparticles (83). Since then, various chemical and physical methods for the preparation of colloidal metal particles were reported until in the 1951 when Turkevitch began fabricating Au-NPs using different methods and employing transmission electron microscopic (TEM) investigations in an attempt to improve the preparative conditions, which led to the development of the Turkevitch method (89) that is still used today for gold nanoparticles synthesis.

The Lee-Meisel method (90) is a common technique used for the preparation of Ag-NPs. It is different from the Turkevitch method in the sense that silver nitrate ($AgNO_3$) is used as a metal source in the Lee-Meisel method. Nowadays, the synthesis of silver nanoparticles is achieved by the reduction of $AgNO_3$ to neutral silver atoms in liquid

chemical methods (91). A typical example; is the use of microwave illumination to thermally facilitate the decomposition of citrate ions in order to give rise to aqueous electrons and citrate^{3-} oxidation products such as; acetone-1,3-dicarboxylate and CO_2, as illustrated in figure 16 below (1,92). The citrate^{3-} oxidation mechanism for the facilitation of nucleation of Ag^+ by irradiation as proposed by Park *et al.* (92) is demonstrated in the flowchart below. Citrate has the ability to serve both as a reducing and stabilizing agent. It is proposed that electrons are donated from citrate^{3-} which consequently results in the formation of Ag-NP seeds that function as catalysts for further reduction of Ag^+ and for the decomposition of citrate^{3-}. The transfer of electrons from citrate^{3-} is attributed to the rapid reduction of Ag^+ to nanoparticle clusters.

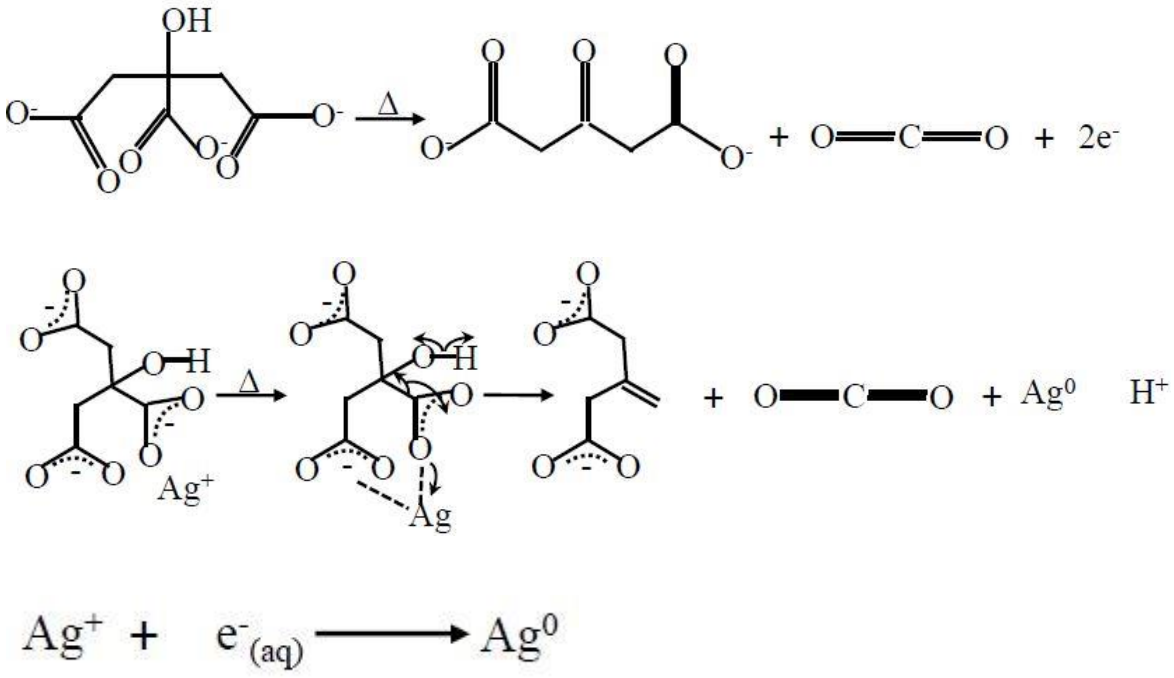

Figure 16. 'Flowchart of citrate^{3-} oxidation, silver ion reduction and nucleation of an Ag^+ precursor by aqueous electrons, respectively' (1: p.58).

The solution becomes supersaturated as more and more silver atoms are formed. As a result, silver slowly begins to precipitate in the form of sub-nanometer particles. The silver atoms that are formed from this point tend to stick to the existing particles, and if the solution is vigorously stirred, fairly uniform particles sizes will be formed. To avoid nanoparticles from combining, a suitable stabilizing agent (in this case; dibutylamine) is added to the solution which sticks to the surfaces of Ag-NPs. Different organic ligands may be introduced into the silver-NPs solution to produce organic-inorganic hybrids with advanced functionality. Moreover, as small clusters aggregate, propagation is induced and a stabilizing agent is added to terminate the process, as shown in figure 17 (1).

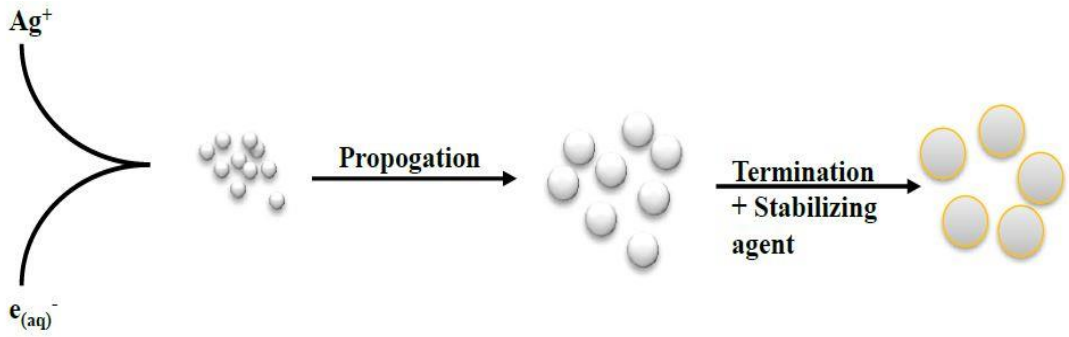

Figure 17. 'Stages of Ag-NPs fabrication' (1: p.59).

2.5. Methods for the synthesis of Ag nanoparticles

After a global outcry on the use of toxic chemical products and processes that generate environmental-threatening substances, there has since been a call to collectively stop or minimize the generation of hazardous substances that end-up in our environments. In an effort to answer to this call, a field of Green Chemistry was adopted in 1990s as an area of study that looks at the development of environmentally friendly processes (93). In light of the above, it is, therefore, empirical that the synthesis of silver

nanoparticles (Ag-NPs) in our case be conducted based on the green chemistry standpoints. According to green chemistry perspectives, the production of Ag-NPs should involve three major steps, which are; (a) selection of solvent medium, (b) selection of a reducing agent and (c) selection of nontoxic substances for Ag-NPs stability. The three main green chemistry steps which are recommended for the synthesis of Ag-NPs have been utilized in this study.

Although there are various synthetic methods of preparing Ag-NPs such as; physical and wet chemical synthetic methods, chemical reduction in solution appears to be the most preferred synthetic technique for the generation of Ag-NP colloids (94). Literature has that the ancient methods of preparing solutions of very fine metal particles are still used today as reference methods with which emergent synthetic techniques are benchmarked (95). In particular, the Lee-Meisel method stands as the most widely used technique for the preparation of Ag-NPs suspensions. However, this method is associated with challenges in particle-size control, claims Creighton *et al.* (96).

In order to take control of the particle size during the metal nanoparticles synthesis, the Creighton method (96) could be adopted. This method has been proven to yield smaller particles of narrow size distribution (< 10nm). Moreover, this very synthetic technique, and of course depending on the reduction potential of the source ion, could be used for the production of nanoparticles of metals such as; Ni, Pt, Cu, etc. Both, the Lee-Meisel and Creighton method discussed above, involve the reduction of Ag ions to metallic silver as well as the chemical or physical adsorption of ligands on the

surface of Ag-NPs in order to inhibit particle coagulation and precipitation, argues Daniel *et al.* (1). The following section will discuss briefly how Ag-NPs are formed through ion reduction, and how particle growth can be monitored using stabilizers and appropriate solvents.

2.6. Reduction of silver ions to metallic silver

Amongst all metal-nanoparticles synthetic routes, the wet chemical method has been used in this study as a synthetic technique for the preparation of Ag-NPs. Thus, it is necessary that we comprehend the mechanism by which metallic silver is produced. To synthesis Ag-NPs suspension, literature claims that one has to start off by, for example, preparing a solution of silver nitrate ($AgNO_3$), silver nitrate dissociates into Ag^+ and NO_3^- upon dissolution and exists as such in solution.

To convert silver ions into metallic silver, a reducing agent is used as an electron donor that supplies an e^- to Ag ion thereby resulting in the production of neutral silver solution. A typical example is one demonstrated by Pastoriza-Santos and Liz-Marzan (97). The duo prepared silver nanoparticles by reducing silver ions with *N, N*-dimethylformide in the presence of water (solvent) and a synthetic hybrid inorganic-organic compound as a stabilizer. A stabilizer is described as a substrate, in most cases, a donor ligand, or a surfactant or a polymer that serves as a protective agent that forms a layer around forming metal-nanoparticles. This shell stabilizes particle growth and subsequently inhibits agglomeration of particles. It also helps retain particles' surface properties (98).

The effectiveness of a given stabilizer is linked with the characteristics of the solvent to be used alongside. The solvent is pronounced to be appropriate if it allows the stabilizer to protrude on the particle' surface, and vice versa if the solvent makes the stabilizer to fall off from the surface of the particle (99). Technically, the stabilizer supposed to completely cover the surface of each particle in solution to avoid polymer-polymer interpenetration. If, for example, two particles in solution are not fully shielded by the stabilizer, they may cuddle together, resulting in a formation of a larger particle whose length is outside the nanometer scale (98). The preparation of Ag-NPs, alike requires a protective agent for stabilization and for precluding nanoparticle coagulation. Therefore, dibutylamine has been used in this study as a stabilizer.

Another way of reducing silver ions to metallic silver and of controlling particle growth is by using a suitable solvent. A solvent is chosen based on its polarity/non-polarity properties and whether the solvent is falling under the protic or aprotic category. The decision on the type of solvent to use is solely determined by the nature of the particle-surfactant or polymer (100). For instance, if particles which are covered with polar surfactants/polymers are prepared in the presence of a polar solvent such as water, these polymers would pile together on the particles' surface so as to reduce the contact surface where polymers meet water. These kind of reactions yield large metal-nanoparticles, which is not what we intend to achieve. To make the polymer spreads away from the particle surface, a non-polar solvent such as ethanol, methanol or ethylenglycol should be used. This study utilized ethanol as a solvent for the synthesis of Ag-NPs. All in all, a successful production of metal-nanoparticles is indicated by the ability to produce a solution that has a uniform particles distribution, and one that is highly stable (101).

2.7. Methods for fabrication of Ag/TiO_2 surfaces

Generally, the surface of a material defines its functions. In view of the foregoing, coating different substrates with thin films could save resources than having to produce the whole body with the functional material, suggests Nagai *et al.* (102). The development of thin films with various thicknesses has not only attracted considerable attention in research, but also in the industry. This is because thin coatings have a wide range of practical applications, ranging from self-cleaning ability to photo-induced bacterial killing ability.

There are various methods developed for the fabrication of thin films, including physical techniques and chemical methods (103) . Amongst many thin films synthetic methods, stand Physical Vapor Deposition (PVD) and Chemical Vapor Deposition (CVD) as the most widely employed techniques in the fabrication of thin coatings (102). CVD and the sol-gel methods are way more economical as compared to PVD methods. Therefore, the former are commonly used (104,105). The subsequent section 2.7.1, discusses in detail the most adopted wet chemical method (sol-gel) for the syntheses of metal-NPs/TiO_2 surfaces which has so far been extensively reported in literature. It also highlights on the most recent developed method (MPM) of preparing Ag-NPs/TiO_2 composite thin films.

2.7.1. Sol-gel method

This synthetic route involves the use of metal/organic polymers to produce coatings on ceramic and glass substrates (106–111). A typical sol-gel procedure starts off by producing a solution composed of a metal alkoxide, acetylacetonate, carboxylate, as well as some soluble inorganic compounds (112–114). Water and alcohols are used as

additional starting materials for hydrolysis and for dissolution, respectively. In addition, an acid or base is employed as a catalyst in this method. Hydrolysis and polycondensation of metal compounds at ambient temperature yields a sol in which colloidal particles or polymers are suspended without precipitation. An additional reaction leads to a wet gel that contains water and solvents (alcohol). To dry the gel, solvents are evaporated, thereby producing microstructures of inorganic composites, glasses and ceramics, after the gel is treated at high temperature to eliminate organic matters.

2.7.2. Molecular Precursor Method (MPM)

This is a novel wet chemical process that requires heat-treatment of samples to remove organic ligands from metal compounds for the fabrication of thin films of crystallized oxides or phosphates and which contain relatively high unprecedented amounts of metal nanoparticles (17,61,115–122). Nagai *et al.*(102) had demonstrated the significance of heat-treatment in the MPM. They reported that surfaces prepared by the MPM have the potential to be developed into commercial products. Furthermore, this method can be used to fabricate highly conductive Ag-NPs/TiO_2 composite thin films and several other metal oxide films with up-to 80 mol% (1) of metal nanoparticles in their matrixes which demonstrates its broad utility. Generally, this method involves the engineering of metal complexes in coating solutions with outstanding stability, homogeneity, miscibility and coatability.

In the MPM, highly stable metal complex anions are dissolved in volat2ile solvents by reacting them with suitable alkylamines. This results in precursor solutions that tend to form excellent amorphous films, just like those formed by the sol-gel method. According to Nagai *et al.* (102), the resultant crystal size of the oxide particles produced by the MPM is smaller than those synthesized by the conventional sol-gel method. The size of the crystallites generated from the MPM is ascribed to the nucleation process of crystallized metal oxides. In a typical metal nanoparticle/titania composite material synthesis, it is preferred that the crystallite size of metal particles be smaller. For this and many other reasons herein above, the MPM has been adopted in this study as a method of fabrication of Ag-NPs/TiO_2 composite thin films.

2.8. Mechanism of photo-activity of pure TiO_2, Metal doped-TiO_2 and Nonmetal-doped TiO_2

A photocatalytic mechanism begins when TiO_2 absorbs a photon (hv_1) with energy equal to or more than that of the band gap of TiO_2 (3.2 eV). An electron (e^-) is excited from the valance band (VB) to the conduction band (CB) of the semiconductor, thereby leaving a positive hole (h^+) on the valence band. Electrons and holes can recombine to release energy in the form of heat, or could get trapped in metastable surface states or react with electron donors and acceptors which are adsorbed on the surface of TiO_2, these cause inadequate photocatalysis.

Trapped electrons and holes may react with atmospheric water and oxygen to form some reactive oxygen species (ROS) such as hydroxyl radical (·OH) and superoxide anions (O_2^-) as demonstrated in figure 18 below (41). These resultant reactive oxygen

species could participate in further photocatalytic reactions, for instance, in the killing of microorganisms. In visible light responsive Ag-NPs-doped TiO_2, the dispersion of metal nanoparticles in the titania matrix produces a new energy level, hv_2 (figure 18) in the band gap of TiO_2 which facilitates visible light absorption by the material (49). Doping of TiO_2 with Ag-NPs does not only reduce the band gap of the semiconductor, but also results in improved trapping of electrons which inhibits electron-hole recombination during illumination. This is attributed to the creation of resonant surface plasmon (SPR) of Ag (123,124).

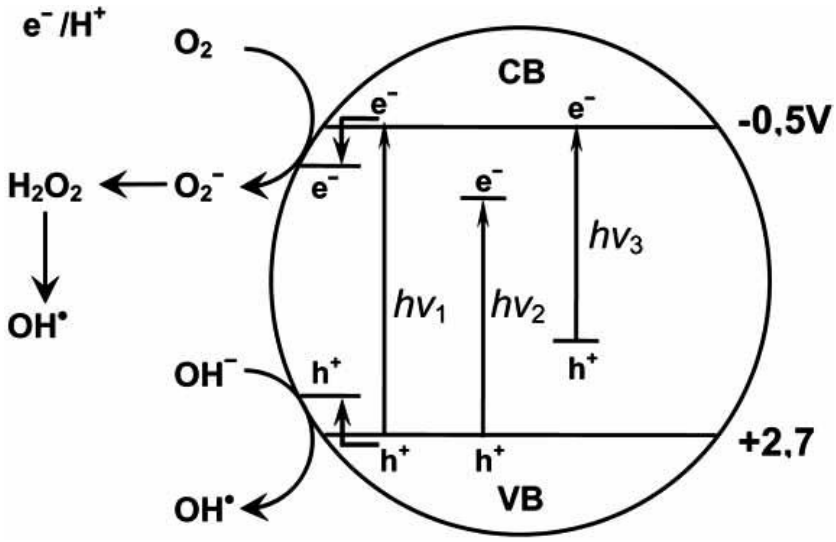

Figure 18. 'Photocatalytic mechanism of bare TiO_2 (hv_1), Ag-doped TiO_2 (hv_2) and non-metal doped TiO_2 (hv_3)' (68: p.157).

CHAPTER 3: RESEARCH METHODS

This section will cover in detail the methodologies that were employed for thin films fabrication and in studying their antibacterial activities.

3.1 Research design

This study was conducted in the order illustrated by the flowchart below.

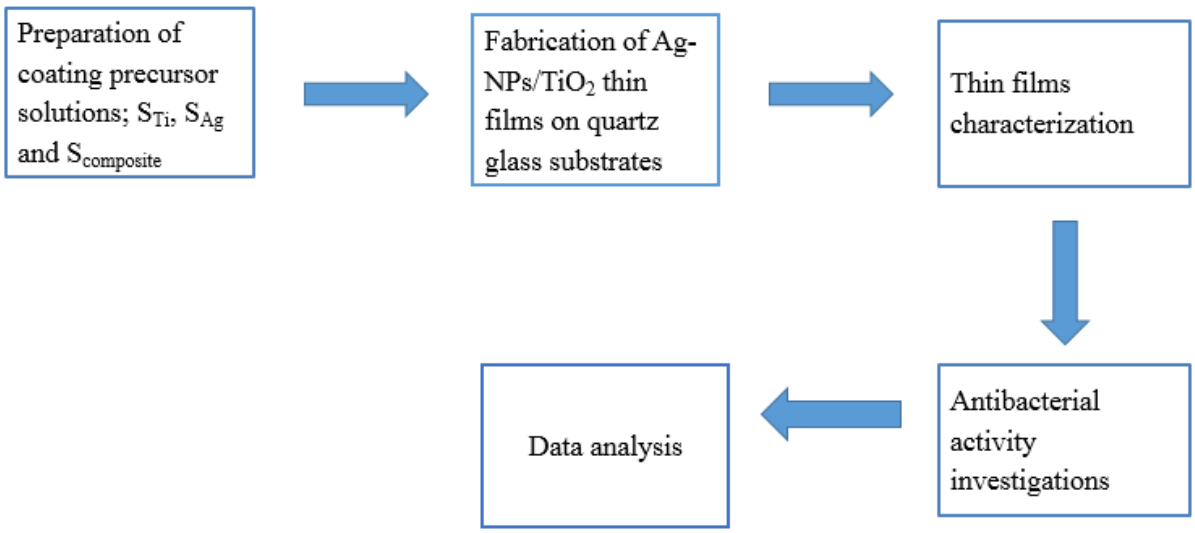

Figure 19. Research design flowchart

3.2. Materials

Chemicals and glassware used in this research were purchased from Genmed Namibia, quartz glass substrates and the spin coater were outsourced from Akishima Glass Co., Ltd in Japan. Thin film samples were sent out for various analyses except for UV/Vis which was done in Namibia. Table 1 and Table 2 (appendix I), show reagents and materials that were used in the preparation of precursor solutions and in the antibacterial susceptibility testing of thin films.

3.3. Procedures

The procedures for the preparation of the two precursor solutions (S_{Ti} and S_{Ag}), the composite solution and for the fabrication of thin films of various concentrations were adopted from the work of Nagai *et al.* (102) as well as that of Daniel *et al.* (1,17).

3.3.1. Cleaning of quartz glass substrates

After the glass substrates were cut in pieces of 2.5cm x 2.5cm or 1.0cm x 1.0cm, a substrate cleaning procedure developed by Daniel *et al.* (1) was adopted in this study for the cleaning of supportive glass surfaces to ensure that they were free of any metal, ionic contaminants as well as organic matters. Firstly, substrates were washed with a solution of detergent and distilled water which was prepared in a ratio of 1:19. They were then rinsed several times with deionized water. Following the preceding step, the glass substrates were then placed in a 1000 ml beaker containing about 500 ml of isopropanol. The beaker was then placed in an ultrasonic bath to eliminate organic and inorganic impurities that could be adsorbed on the surfaces. The glass wavers were then removed from the beaker and placed on a clean glass tray and dried at 70 °C.

3.3.2. Preparation of the Titania precursor solution (S_{Ti})

A highly stable solution of titania was produced by reacting the Ti^{4+} complex of EDTA with dibutylamine in a mixture of ethanol and methanol which served as solvents. The mixture was then heat-treated by refluxing under the fume hood. After refluxing, it was cooled to room temperature, and hydrogen peroxide was added. The solution was refluxed further allowed to cool down to room temperature. Figure 20 below summarises briefly the specific amounts of reagents and procedures involved in the synthesis of the titania precursor solution.

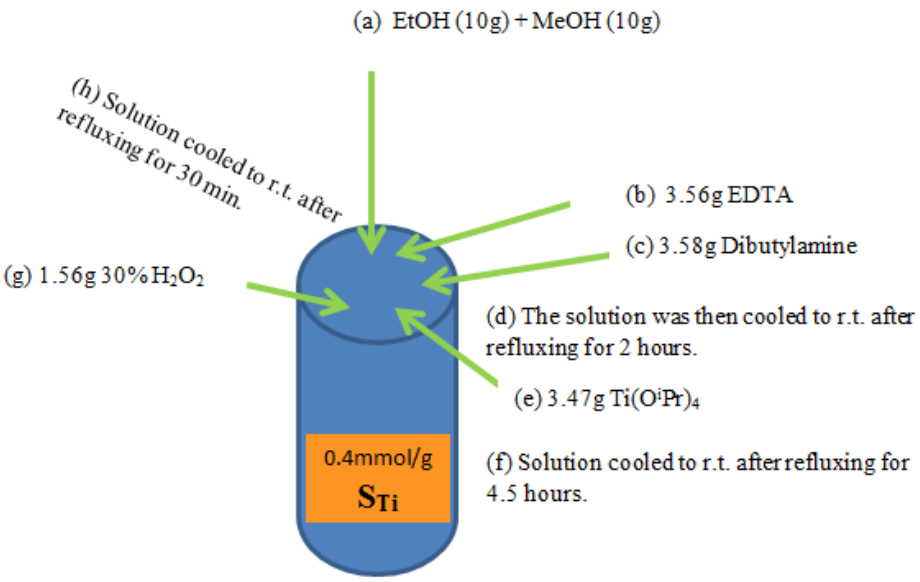

Figure 20. Schematic representation of procedures for the preparation of the titania precursor solution.

3.3.3. Preparation of the silver precursor solution (S_{Ag})

Prior to the preparation of the silver solution, the light in the room was minimized by switching off some of the light sources and the solution was then prepared in an Amber glass bottle (brown in colour) to prevent silver acetate from decomposing when exposed to ambient light in the presence of ethanol (125). Thereafter, the solution was utilized immediately after it was prepared. The procedures on how the S_{Ag} was prepared are outlined in figure 21 below.

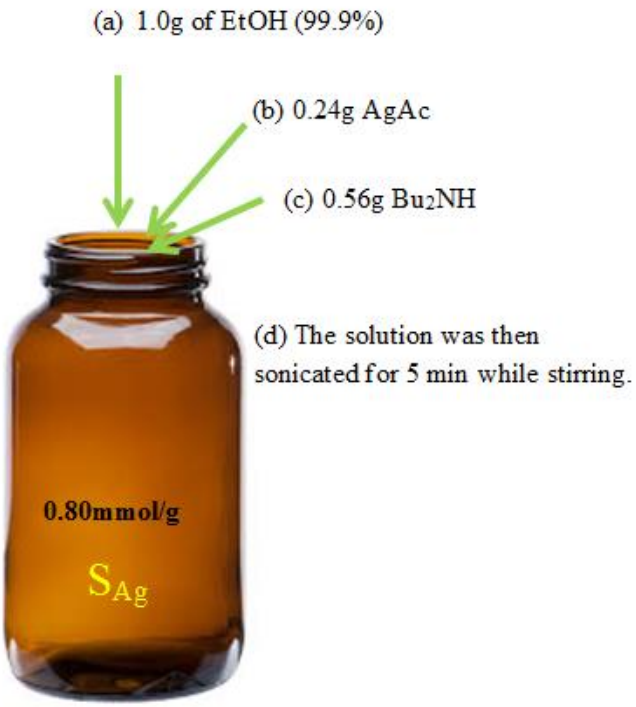

Figure 21. Schematic representation of procedures for the preparation of the silver precursor solution.

3.3.4. Preparation of Ag-NPs/ Titania composite precursor solutions and thin films

The Ag-NPs/TiO_2 composite solutions of various concentrations were prepared, for example, for 50% Ag; a 1.0g of silver solution was added to 2.0g of titania solution, depending on the required concentration of Ag in the final composite solution. Following mixing, the composite solution is sonicated with stirring for 5 min for achieving maximum homogeneity. The Ag-NPs/TiO_2 composite thin films were fabricated by pipetting a 100µl or 1.0 ml of the composite solution on a1.0 m^2 or 6.25 m^2 glass substrate, respectively. The substrate was then coated by spinning using a spin coater that is set to a double step mode. The first step runs at 500 rpm for 5 seconds and the second step runs at 2000 rpm for a period of 30 minutes. Immediately after

coating, the coated glass waver was heat-treated at 600 °C for 30 min. These procedures were repeated for every substrate of a distinctive concentration. Figure 22 below summarizes these procedures.

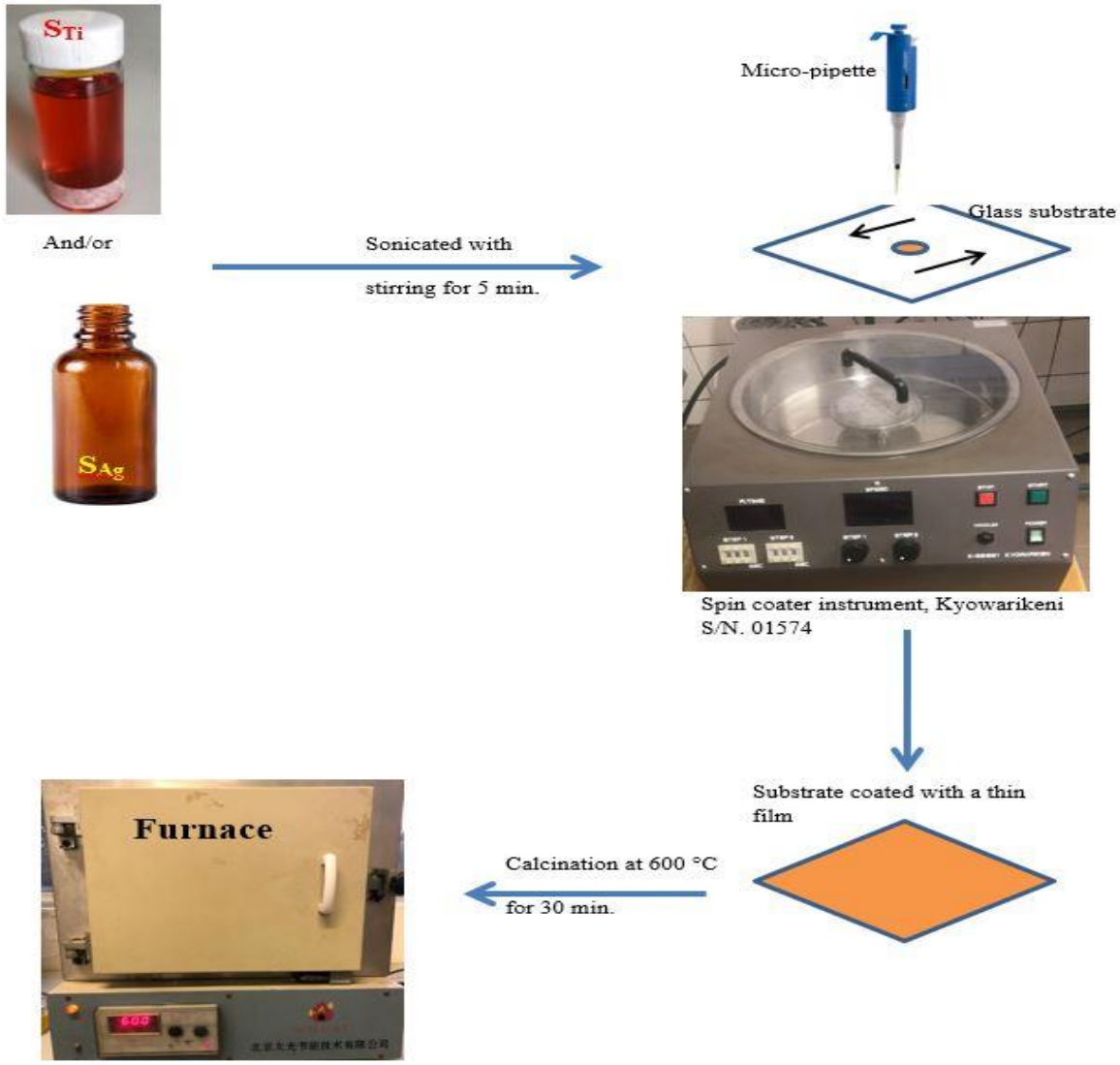

Figure 22. 'Fabrication of thin films on quartz glass substrate using the spin coating system' (2: p.107).

3.3.5. Thin film characterization

Thin films used in this study were characterized as follow; phase formation and crystalline structures of films were determined by X-ray diffraction (XRD) at Botswana International University of Science and Technology (BIUST), Palapye, Botswana. An X-ray diffractometer (MXP-18 AHF22, Bruker AXS) with Cu-Ka rays generated at 45 kV and 300 mA, and which has a parallel beam optic with an incident angle of 0.3º was used in this study for phase identification and crystalline properties investigations.

The scanning electron microscopy (SEM) was chosen to be the characterization technique for the assessment of the surface morphology of thin films because SEM, unlike light microscope, allows a large amount of the substrate surface to be focused and observed at once (17). Top view and the cross-sectional images of the resultant films were taken using an S-4200, Hitachi field emission scanning electron microscope at an accelerating voltage of 5.00 keV. The cross-section of the thin films was coated with gold colloids through sputtering to enhance conductivity of the films. This was also conducted at Botswana International University of Science and Technology.

Figure 23. Photograph of the field emission scanning electron microscopy (FE-SEM) at BIUST.

The most used tool for a thin film thickness measurement is the stylus profilometer (126). In this study, a Sloan DEKTA3 profilometer was employed. In order to traverse the breadth of a 15 mm x 25 mm film, the travel length was set to 25 mm to ensure that both sides of the height of the film were accounted for. Below is a photograph of the profilometer instrument (figure 24).

Figure 24. A photograph of a Sloan DEKTA3 profilometer.

The optical absorptions of the films were obtained by using a Perkin-Elmer Lambda 35 UV/Vis spectrophotometer in the wavelength range of 200 nm – 800 nm, using the double beam mode. Detailed procedures are found in a paper by Daniel *et al.* (17). Figure 25 shows the photograph of the UV/Vis spectrophotometer that was used in our lab for the study of the optical properties of the fabricated thin films.

Figure 25. Photograph of the Perkin-Elmer Lambda 35 UV/Vis spectrophotometer.

3.3.6. Antibacterial activity evaluation

The antibacterial activity of representative thin film glass substrates against *E-coli* (ATCC 25922) was determined by two different methods; (a) Disk Diffusion Method (127) and the (b) Viable Cell Count Method (9).

a) Disk Diffusion Method

Prior to the antibacterial experimentations, all glassware and substrates were sterilized in an autoclave at 121 °C for 15 min. For the zone of inhibition test, about 25 ml of the liquid Müeller-Hinton Agar was poured onto disposable sterilized Petri dishes and allowed to solidify. Then 100 µl of the *E. coli* culture containing approximately $1x10^8$ CFU/ml, which was adjusted to the 0.5 McFarland standard prepared using protocols by Lalitha (127) was pipetted onto the agar and spread uniformly using a sterilized spreading rod. Thin film samples of concentrations ranging from 10 mol% Ag – 100 mol% Ag ware gently placed over the inoculated agar gel. Plates were then incubated with illumination or in the dark at 37 °C for 24 h and the antagonistic activity was depicted by a clear zone of inhibition around the coated substrate. Zones were measured to the nearest whole millimetre, using a ruler. Uncoated glass wavers were

also tested for antibacterial activity as negative controls. The standard antibiotic gentamicin (50µg/ml) was used as a positive control.

b) Viable Cell Count Method

To evaluate the antibacterial activity of thin films, representative films were investigated both in the dark and under visible light supplied by a fluorescent lamp, 60 W. The light intensity on the films' surface was $1.2x10^3$ lux. Each representative film (area = 6.25 cm^2) was placed in a sterilized Petri dish, then 1000 µl of the *E. coli* culture of 1/1000000 ($1x10^{-6}$ cells/ml) dilution factor was pipetted drop-wise onto the coated surface of each film. The Petri dish was sealed and illuminated with visible light. The illumination density was recorded using a light meter Pro application. The irradiation distance between films 'surface and the lamp was 12 cm, films were light-treated for a period of 3h. To measure the activity in the dark, the experiment was carried out under similar conditions but without illumination.

For easy and correct counting of survival *E. coli* cells, the bacterial containing drops from the surface of each film were washed off by using 9 ml of sterile tryptic soy broth in sterilized Petri dishes. Then a 100µl of each bacterial suspension was dispersed on the plate count agar. The plates were then incubated at 37 ºC for 24 hr. The number of surviving *E. coli* colonies on every Petri dish per film concentration was counted using a colony counter. The counts on three plates corresponding to a particular sample were averaged. The very same procedures were employed for the blank glass control. Figure 26 below summarizes the antibacterial evaluation procedures of thin films by the viable cell count method.

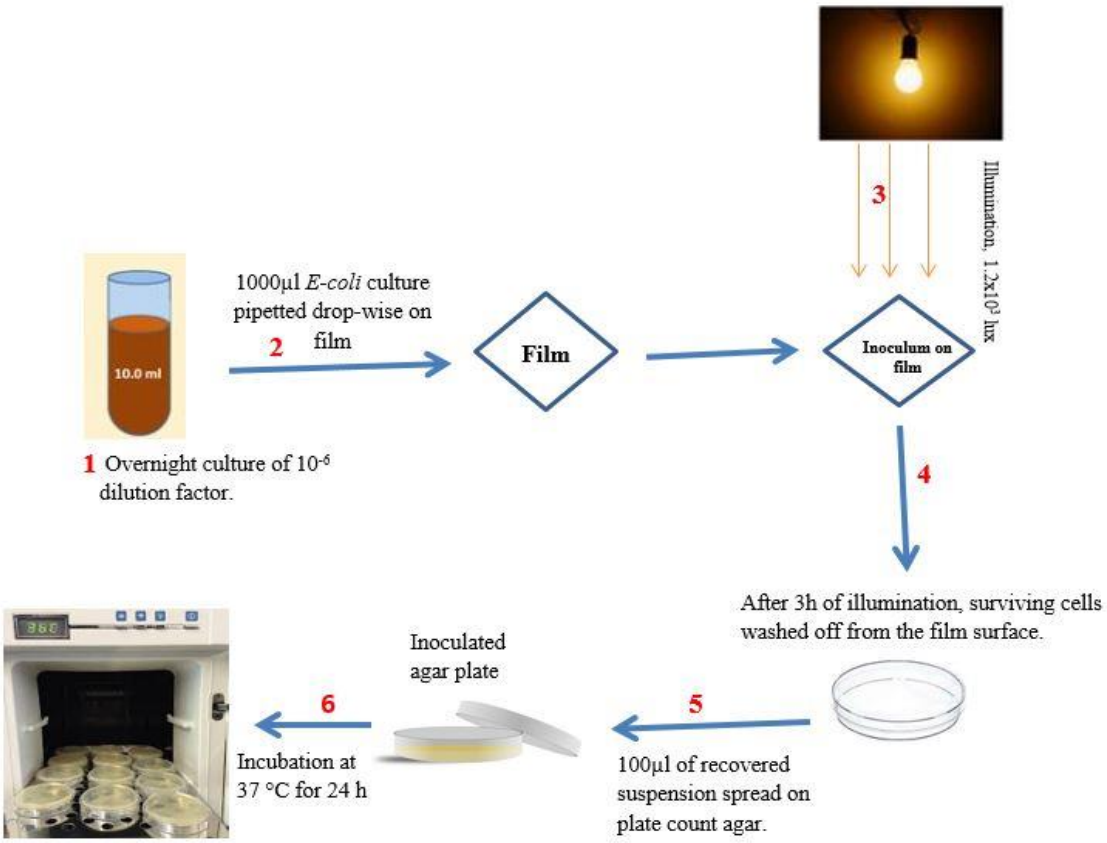

Figure 26. Antibacterial evaluation procedures of Ag-NPs/TiO_2 thin films (Viable Cell Count Method).

CHAPTER 4: RESULTS AND DISCUSSIONS

4.1. Synthesized precursor solutions

A stable coating solution of titania with an intense orange-red colour was prepared. According to Nagai and Sato as cited by Daniel *et al*. (1), this colour is ascribed to the Ti^{4+} complex coordinated with the H_2EDTA^{2-} and the peroxo ligand. It is these very ligands that enhance the stability of the titania solution, as reported by Nagai and Sato (102). Structural analysis of the EDTA complex formed in the solution reveals that the coordination nature of EDTA ligand in the complex ion is 5 which results in a precursor complex having not only a high stability but also an excellent homogeneity, miscibility and coatability. These properties allow the titania solution to be stored for a long period of time and utilized when needs be.

The silver precursor solution was immediately used after it was prepared to avoid decomposition of silver acetate upon exposure to ambient light in the presence of ethanol (125). The two solutions were mixed at different molar concentrations to fabricate films with various concentrations of Ag-NPs in the titania matrix. Photographs of the two resultant precursor solutions are shown below in figure 27.

Figure 27. Photograph of a 0.4mmol/g TiO_2 (left) and 0.8mmol/g Ag-NPs (right) precursor solutions.

4.2. Fabricated thin films

Optically transparent to opaque, crack-free and reproducible films of bare TiO_2 and Ag as well as composite films of Ag-NPs/TiO_2 of various molar concentrations were fabricated on $1cm^2$ or $3.25cm^2$ quartz glass substrates. The molar concentration of silver nanoparticles content in the composite films varied from 10 mol% - 90 mol%. The relation between the physical appearances of the composite films with respect to their colour with the Ag-NPs content in the TiO_2 matrix is that the colour ranged from clear to dark as the Ag-NPs content in the matrix increases. Both the bare Ag-NPs and TiO_2 were clear in colour. Figure 28 shows some of the fabricated thin films of different concentrations.

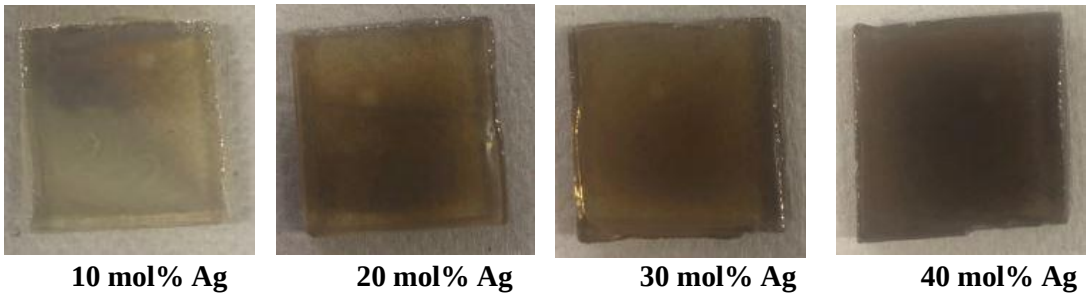

10 mol% Ag **20 mol% Ag** **30 mol% Ag** **40 mol% Ag**

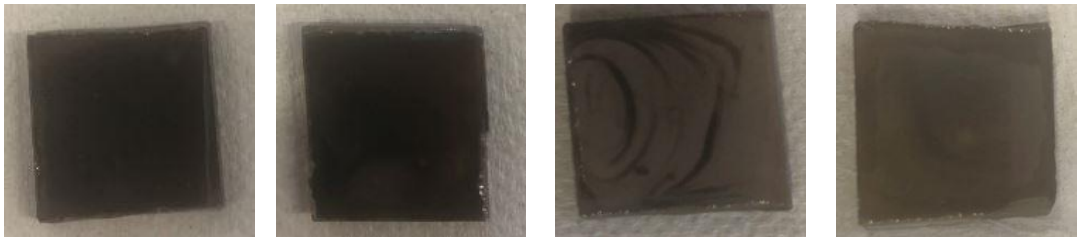

50 mol% Ag **60 mol% Ag** **70 mol% Ag** **80 mol% Ag**

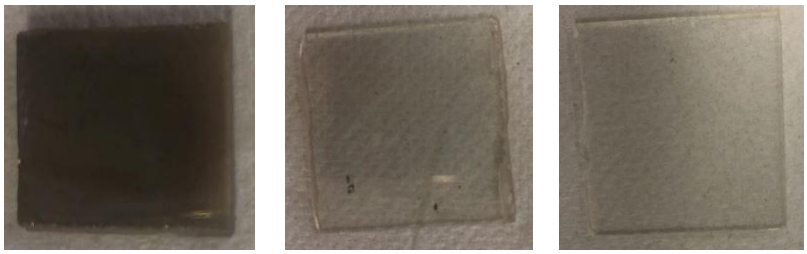

90 mol% Ag **Pure Ag** **Pure titania**

Figure 28. Photographs of fabricated thin films with different concentrations of Ag-NPs.

4.3. Structural and chemical characterization of thin films

4.3.1. Phase analysis

Figure 29 shows the XRD patterns of TiO_2 and Ag-NPs/TiO_2 composite thin films after calcination at 600 ºC for 30 min. In the case of pure TiO_2, both phases (anatase and rutile) were observed at 25.0º, 38.2º, 44.4º, 64.6º and 77.5º. These peaks indicate that the neat TiO_2 films fabricated consisted of a mixed-phase of anatase and rutile, known to have greater photocatalytic activity than an individual pure anatase or rutile

phase (8). Only the MPM is known to fabricate a mixed phase TiO_2 film at temperature less than or equal to 600 °C (102).

For Ag-doped Titania (80 mol% Ag), a typical anatase phase corresponding to peak 110 appeared at 25.1º. The 80 mol% Ag film clearly exhibits the diffraction peaks, i.e. 200, 220, and 311 of the metallic silver, it also showed a face-centred cubic structure (fcc) of metallic silver. For pure Ag, a peak 110 shows that after calcination, there was an insignificant amount of silver oxide present and detected in the film. According to Daniel *et al*. (1), the silver oxide in the pure Ag film might had formed during cooling in air, where Ag might had reacted with atmospheric O_2. Moreover, it was observed that the intensity of the diffraction peaks 111 and 200 of Ag phases increased as the content of Ag-NPs in the titania matrix increased. A decrease in the intensity of 101 and 111 diffraction peaks of the TiO_2 was realized as the silver content in the titania matrix was increasing. The mean crystal size of the resulting Ag-NPs was around 10 nm determined by using the Scherrer's equation on the wide-angle XRD peak broadening analysis at the 200 peak (3).

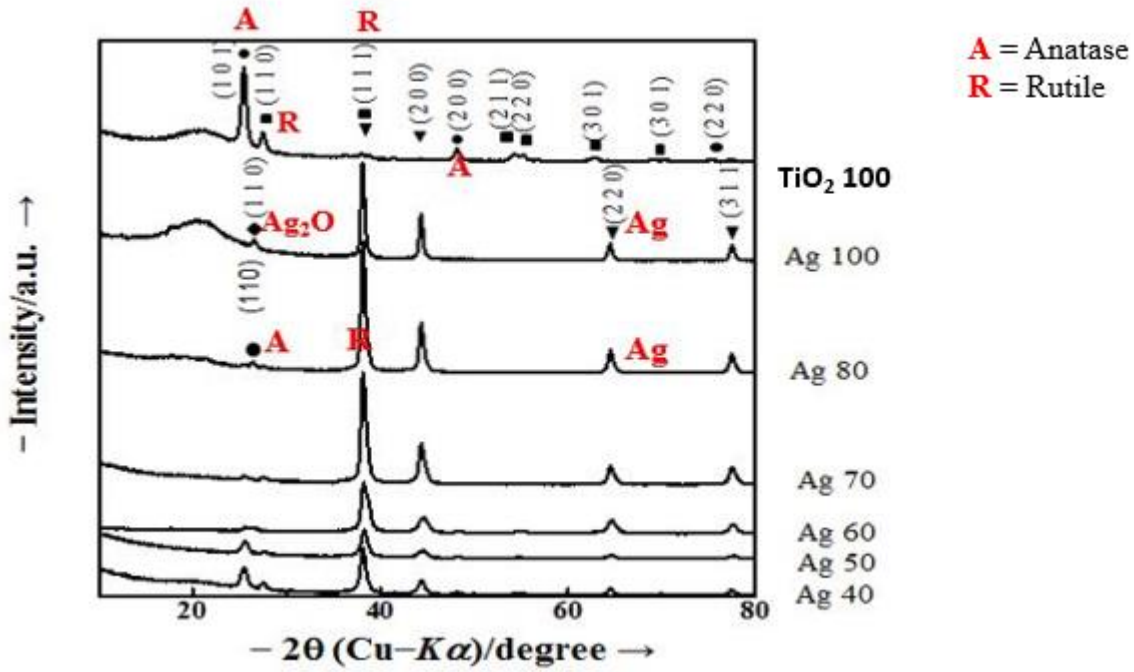

Figure 29. Wide-angle XRD patterns of the prepared thin films

4.3.2. SEM analysis

To obtain Ag, TiO_2 and resultant composite films that can be reproduced, the optically transparent to dark crack-free films were prepared. The calcination temperature of 600 ^oC was selected as the optimum temperature for the fabrication of Ag-NPs/TiO_2 composite thin films (17). Heat-treatment at 600 ^oC yields films that contain excellent crystals of mixed phase anatase and rutile TiO_2, which leads to a decrease in the photo-excited electron and hole pairs recombination (1). Therefore, calcination at this temperature increases photocatalytic activity of the material, thereby subsequently enhances the photo-induced bactericidal activity of the thin films (8).

The morphology of thin films seems to be different depending on the Ag content. It can be seen from the low-magnified image of the scanning electron microscopy (SEM) in figure 30 (a) below that the film produced at lower Ag content, i.e. 10 mol% Ag

film contains well dispensed silver nanoparticles with a diameter range of 20 – 30 nm. Figure 30 (b) and (c) indicate FE-SEM images of Ag-NPs/TiO_2 composite thin films with various Ag concentrations. As observed from this figure, the amount of silver particles in the 50 mol% Ag composite films is fewer and particles appear to be uniformly distributed across the film than in the 90 mol% Ag composite (higher Ag concentration) films.

As Ag-NPs load increases, partial agglomeration of silver nanoparticles was observed. In the 90 mol% Ag film, it can clearly be seen that the Ag particles appear aggregated and as the loading of Ag-NPs into the TiO_2 continues, large clusters of particles formed as can be seen in figure 30 (c), same behaviour was observed by Daniel *et al.* (17). Furthermore, instead of having a smooth surface like that of the 10 mol% Ag film, the 90 mol% Ag film displays a rougher surface morphology. The metallic silver looks brighter in the image because Ag, just like other heavy metals backscatter electrons more strongly than light elements (7).

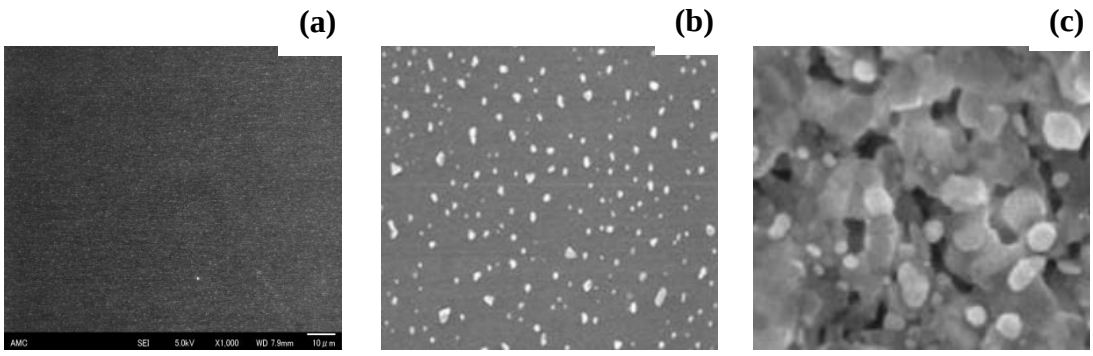

Figure 30. FE-SEM images of (a) 10 mol% Ag, (b) 50 mol% Ag and (c) 90 mol% Ag films.

4.3.3. Profilometry; thin film thickness analyses

Figure 31 (a) shows a profilometric scan for a 60 mol% Ag representative film covering a 25 mm travel distance. As deduced from the profilometric scan data of this representative sample, the average film thickness was 100 nm. The multiple peaks-like structures observed on the scan data denote the degree of film surface roughness which could be attributed to disorganized film growth, which might have caused by the accumulation of silver nanoparticles into the titania matrix (1) as shown in figure 31 (b). Additionally, film surface roughness might have resulted from the presence of moisture possibly incurred during film preparation, which results in porosity in the film (128). Another factor that is ascribed to film surface roughness are gasses that possibly might have dissolved in the film during fabrication (17). Dissolved gasses result in bubbles formation on the film surface thereby consequently results in porosity.

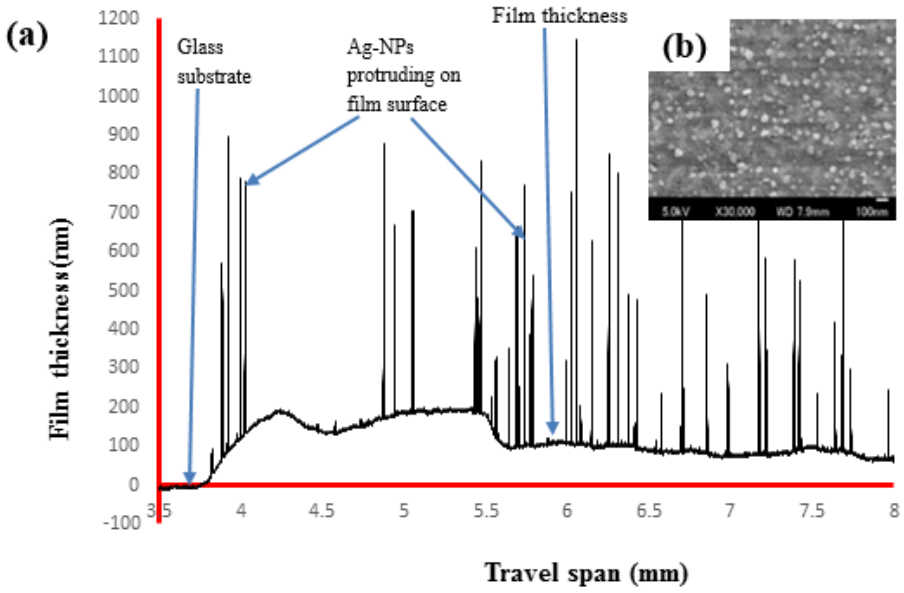

Figure 31. (a) Profilometric scan of a 60 mol% Ag thin film, (b) FE-SEM image of a 60 mol% Ag film.

4.3.4. Optical property of fabricated thin films

Figure 32 (a) shows UV-Vis absorption spectra of bare titania and silver-NPs composite thin films. As can clearly be seen from the these spectra, the TiO_2 film exhibited a low-intensity absorption band in the visible region. Conversely, it was observed that its absorption intensity improved considerably in the ultra violet region. This absorption behavior confirms that TiO_2 is greatly resposive to UV-light and poorly or not at all absorbs in the visible region. While the Ag-NPs film displayed a lower and broad absorption band at shorter wavelength, and particularly showed a peak at around 410 nm. This peak position is attributed to the surface plasmon resonance (SPR) of silver nanoparticles (17). Rochhlz *et al.* (129) reported that 'when a film of Ag-NPs is exposed to visible light, a large oscillatig electric field around silver nanoparticles is generated' (p.11).

In composite thin films of various Ag contents (50 -70 mol%), figure 26 (b), far-reaching absorption across the visible region at wavelenghs > 400 nm was observed in addition to an intense SPR peak that appeared at around 400 nm. The wide range absorption in the visible region observed for composite films is ascribed to the localized surface plasmon resonance (LSPR) of Ag-NPs suspended in the titania matrix (1). As the Ag content increased in composite films, the absorption intensity in the vis-region also increased, except for the 90 mol% Ag film, this very behaviour has been widely reported (130,131). The unsual absorption behaviour of this film could be due to a decrease in the TiO_2 content in the film (17) or possibly due to the presence of high amounts of Ag-NPs in the film which might had covered or blocked the titania surface thereby reducing accessiblity of the material to light and concequently resulted in lower absorption intensity.

Results from figure 32 (b) show that the 70 mol% Ag thin film has the highest absorbance. This impulies that this film exhibits the highest photocatalytic activity, therefore, theoretically it should possess the highest antibactericidal and bacteriostatic activity (36). Another observation was that, although, TiO_2 was successfully doped with silver nanoparticles, its band gap remained the same (17). However, the photocatalytic property of the material increased significantly with an increase in the Ag content.

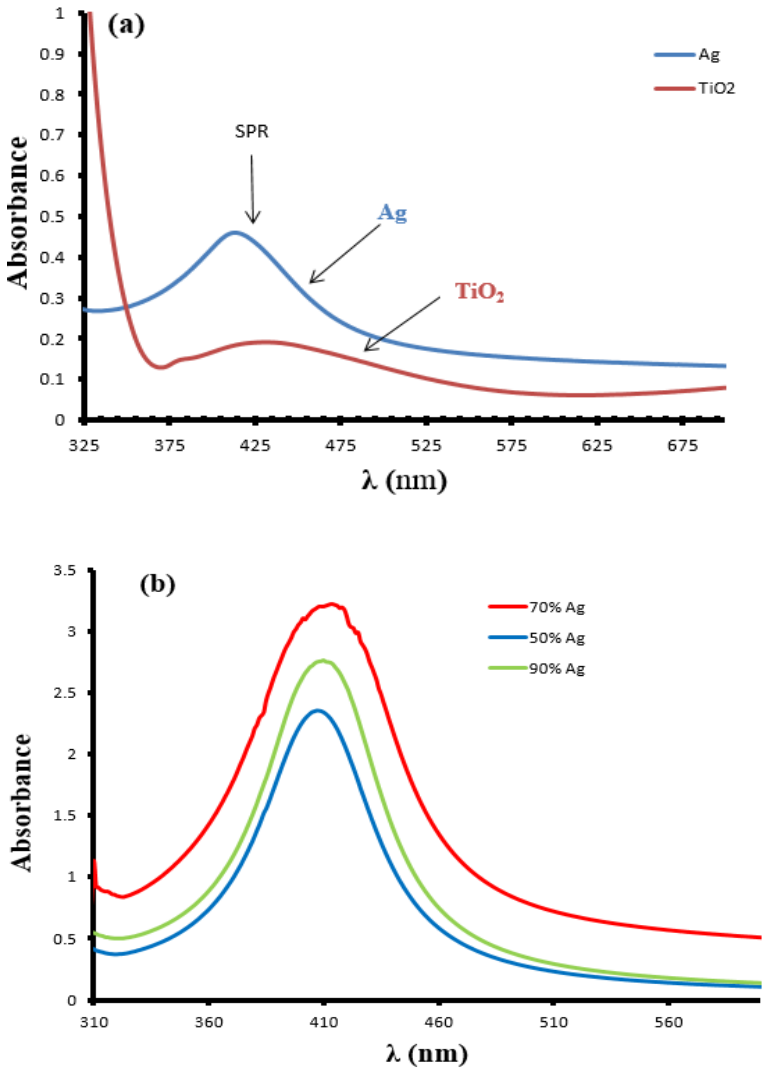

Figure 32. UV–Vis absorption spectra of (a) the a-TiO_2 and Ag-NPs, and (b) composite photocatalyst thin films.

4.4. Antibacterial activity evaluation

4.4.1. Disk diffusion Method

Images in figure 33 show the photo-induced antibacterial activity of the positive control (Gentamycin) and negative control (blank glass waver), pure TiO_2, pure Ag and composite films after 24h of incubation. The antibacterial activity is evidenced by an inhibition zone of *E. coli* growth around resultant substrates as shown in figure 33. The presence and the size of these inhibition zones, which are defined as areas free of bacteria or where bacterial growth is prevented (11), reflect the bactericidal effect of a particular thin film.

Bacterial growth was observed on the top and adjacent to the bare glass waver, which implies that the negative control exhibits no bactericidal activity. No zone of inhibition was observed for pure TiO_2 films under visible light, which clearly confirms that indeed TiO_2 does not absorb in the visible region. Pure Ag films had unclear zones of inhibition. Results from figure 34 shows that all composite films could inhibit bacterial growth under visible light, with the highest inhibition zone recorded for the 70 mol% Ag film with a diameter value of 18.8 mm. Composite film 50, 60, 80 and 90 mol% Ag displayed inhibition zone diameters more less the same as that of gentamicin (15.2 mm).

For the composite films, the diameter of the inhibition zone increased as the Ag-NPs load in the TiO_2 matrix increased. The diameter of the inhibition zone increased from 11.2 mm – 18.8 mm with the increase of Ag-NPs content in the composite films. This trend was not observed for films doped with more than 70 mol% of Ag-NPs. Reasons behind this unusual behaviour might be due to a decrease in the TiO_2 content in the film (17) or possibly due to the presence of high amounts of Ag-NPs in the film which

might had covered or blocked the titania surface thereby reducing accessiblity of the material to light and concequently resulted in lower photocatalytic activities.. The former was expected because the driving force of silver ions diffusion from the bulk to the surface is larger for films with higher silver contents (7).

Ag-only films did not show definite zones of inhibition, and this could be attributed to the fact that Ag appeared as bulk or silver crystal aggregations in silver-only films, which led to very limited silver ions diffusion. While in composite films, Ag appeared as very fine nanoparticles that were well dispersed in the TiO_2 matrix, thus, they exhibited much larger inhibition zones. Composite films with 70 mol% silver loading showed the most notable antibacterial effect and the diameter of the inhibition zones improved by 73% in relative to the 10 mol% Ag film's zone of inhibition. The antibacterial activity of composite films is characteristic of their high photocatalytic property which is further ascribed to the localized surface plasmon resonance (LSPR) of silver nanoparticles observed at around 400 nm in the UV/Vis spectra (1).

The mechanism on the photo-induced bacterial killing has still not been established. Some researchers have proposed that silver might be used as a metal in the deactivation of bacterial cells, however, the active agent appears to be ions produced. In the presence of water and oxygen, silver particles release small amounts of silver ions, which induce cell death (76). On the other hand, Panacek (132) suggested that Ag-NPs might adhere on the surface of the cell membrane, thereby affecting cell activities and consequently results in cell death. The interactions of silver nanoparticles with the bacterium cells depend on the size and shape of the nanoparticles. In this study, bacteria death was probably caused by the leaching of active biocidal Ag ions from the embedded silver nanoparticles present in the composite coating matrix into the surrounding aqueous medium.

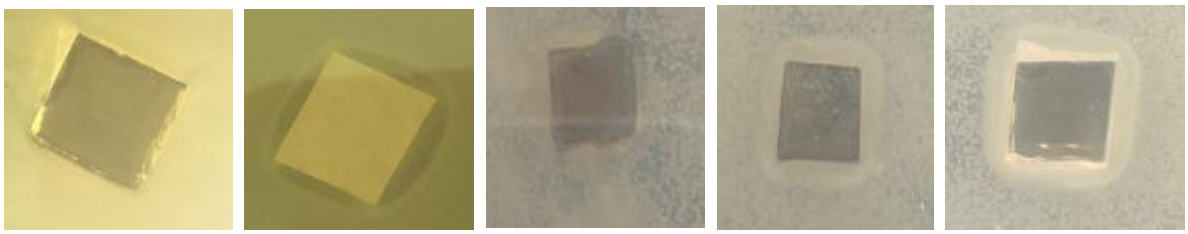

Bare glass + control Pure TiO_2 10 mol% Ag 50 mol% Ag

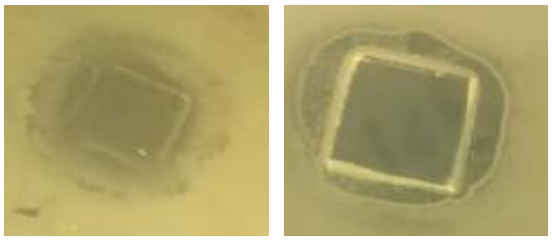

70 mol% Ag 90 mol% Ag

Figure 33. Photographs of zones of inhibition test results of selected thin films

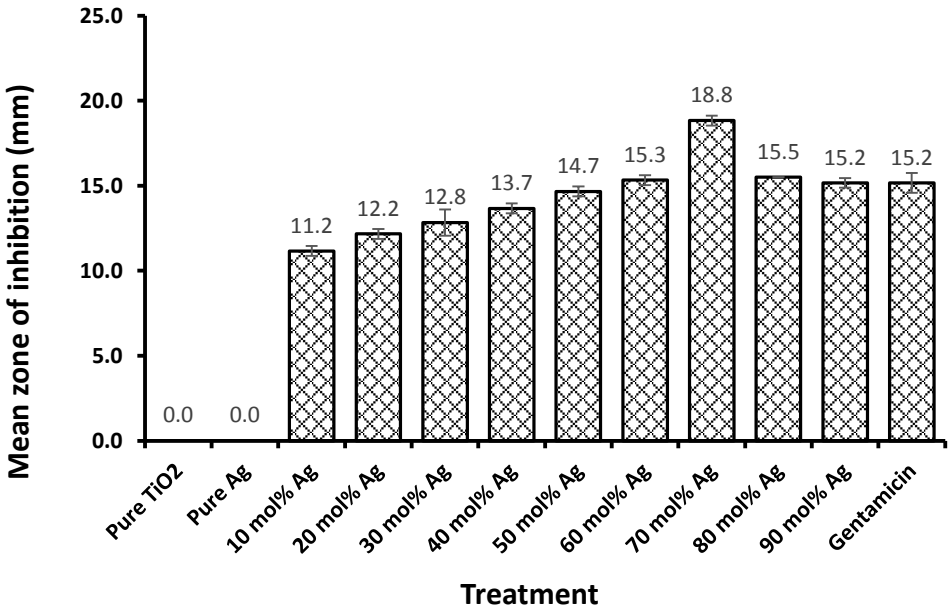

Figure 34. Mean zones of inhibition of films with different Ag-NPs against the zone of the positive control. Means ± standard errors of 3 replicates are presented.

4.4.2. Viable cell count method

Viable cell count tests were also carried out in the dark and under visible light on all representative composite films, including for both the positive and negative control. Figure 35 shows the bacteria killing ratio in the dark and under visible light illumination. After 3h of visible light exposure, all Ag-NPs/TiO_2 composite films exhibited bactericidal activity with different inhibitions of *E. coli* cells. Generally, the composites with richest contents of silver nanoparticles showed the highest antibacterial activity against *E. coli* both in the dark in under visible light. Following films treatment under visible light, the viable count for *E. coli* showed 83% inhibition by the film: 70 mol% Ag, while under the same conditions, pure TiO_2 film showed only inhibition of 3%. In fact, considering that pure TiO_2 does not absorb in the visible region, the 3% inhibition recorded for pure TiO_2 should, therefore, not be ascribed to it. The decrease of the number of viable cells by 3% by the pure TiO_2 film might have been due to natural apoptosis (10).

The film 20 mol% Ag and 30 mol% Ag with less Ag-NPs contents showed lower percentage inhibition of 11% and 26%, respectively. As can be observed in figure 35, pure TiO_2 particles present no bactericidal activity in the dark, indicating that Ag-NPs were the ones responsible for the killing of *E. coli* cells in the dark. The antibacterial effect of Ag-NPs incorporated TiO_2-materials has been extensively reported (47). Moreover, silver ions are also photoactive in the presence of visible light and the photochemical reaction of Ag-cysteine complex hinders the enzymatic function of the affected proteins (membrane proteins of bacteria), leading to enhanced inactivation of bacterial cells (133). The silver-only films showed 5% decrease after 3h of visible light illumination and 3% decrease in the dark, respectively.

In this study, a bare glass was chosen as a blank control. The control results showed about 1% inhibition of *E. coli* cells after 3h of visible light exposure. This could be attributed to the fact that bacteria were exposed to long wavelengths of visible light for a long period of time (3h) which might have damaged the *E. coli* cells by exciting photosensitive molecules within the cell to produce oxygen reactive species which inactivated the cells and ultimately resulted in cell death (7). In the dark, the antibacterial activities exhibited by composite films was very low. While under visible light, activities increased considerably. This indicates that visible light was necessary for enhancing activities. Significant inhibition was observed for the 50 – 90 mol% Ag films both in the dark and under visible light. Furthermore, As the Ag load increased in the film, the bacterial inhibition activity of the material also increased both in the dark and under visible light.

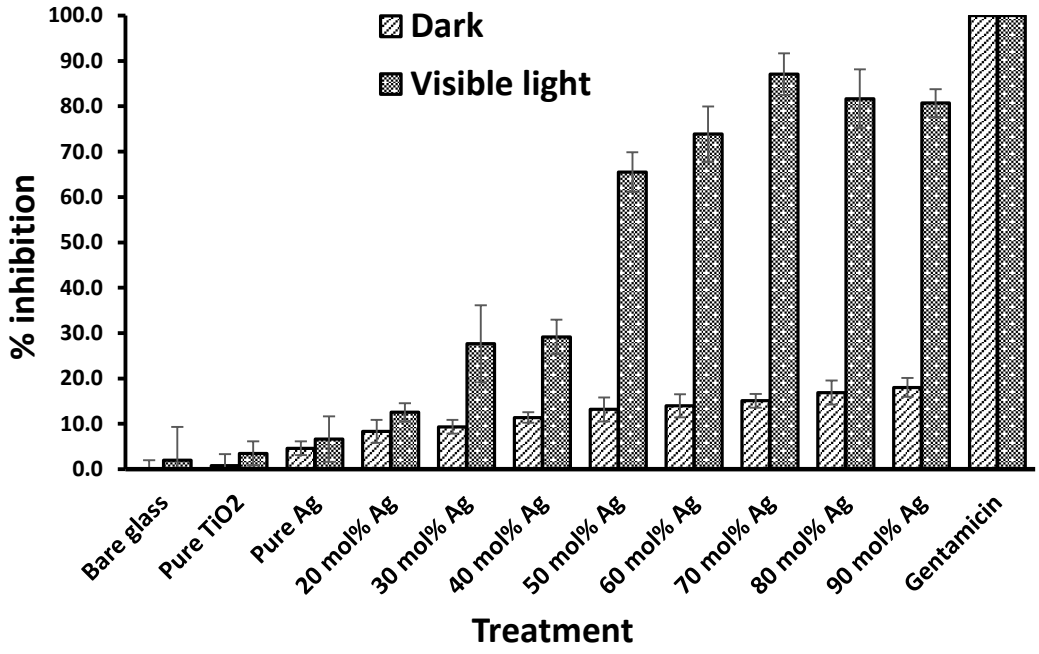

Figure 35. Antibacterial activity evaluation of various thin films in the dark and under visible light. Means ± standard errors of 3 replicates are presented.

CHAPTER 5: CONCLUSIONS AND RECOMMENDATIONS

a) Conclusions

Composite films of various molar concentrations of silver nanoparticles incorporated in the TiO_2 matrix were fabricated on quartz glass substrates using the molecular precursor method (MPM). The prepared films were characterized by employing some analytical techniques for studying different parameters. XRD findings showed that the synthesized films were composed of a mixture of anatase and rutile TiO_2 phases, known to have greater photocatalytic activity than an individual pure anatase or rutile phase. FE-SEM and Profilometry analyses revealed not only the nature of the films' surface morphology but also revealed the film thickness, respectively.

UV/Vis analysis indicated that pure TiO_2 films do not exhibit photo-responsive ability in the visible region. Its absorption intensity, however, increased considerably at shorter wavelengths, proving that pure titania indeed only absorbs in the ultraviolet region. While all Ag-NPs/TiO_2 composite films displayed photo-responsive ability in the visible region, and the photocatalytic activity of films improved significantly as the Ag-NPs load in the titania matrix increased. The visible light-induced responsiveness of the composite films in my study is specially ascribed to the localized surface plasmon resonance of silver nanoparticles observed at around 400 nm in the UV/Vis spectrum.

This study has managed to bridge the gap that existed in literature by having investigated the antibacterial activity of thin films fabricated by the MPM at 600 °C. As in the case of the photocatalytic activity of composite films, the photo-induced

bactericidal effect of the very films increased with an increased in the molar concentration of Ag-NPs in the TiO_2 matrix. The findings from this study have proven that indeed silver nanoparticles were instrumental in enhancing both the photocatalytic and bactericidal activity of composite films under visible light. Therefore, silver can be pronounced as one of the most suitable noble metal dopants for the development of light-cleaning TiO_2-coated surfaces.

b) Recommendations

For the advancement of this work, it is recommended that apart from *E. coli*, other bacteria species be used in the evaluation of bactericidal effect of Ag-NPs/TiO_2 composite films. Another recommendation is the study of the photo-induced bacterial activity of Ag-NPs/TiO_2 films prepared using MPM but heat-treated at temperatures in the ranges of 450 °C – 550 °C. As some researchers have reported that films prepared within 450 °C – 550 °C temperature range tend to contain solely the anatase phase of TiO_2 and as a result they claim that these films exhibited the highest antibacterial activity.

6. REFERENCES

1. Daniel L, Nagai H, Yoshida N, Sato M. Photocatalytic Activity of Vis-Responsive Ag-Nanoparticles/TiO_2 Composite Thin Films Fabricated by Molecular Precursor Method (MPM). Catalysts. 2013;3(3):625–645.

2. Cunha FA, Maia KR, Mallman EJ, Cunha MD, Maciel AA, Souza IP, Menezes EA, Fechine PB. Silver nanoparticles-disk diffusion test against *Escherichia coli* isolates. Revista do Instituto de Medicina Tropical de São Paulo. 2016;58(1):2-4.

3. Liu Y, Wang X, Yang F, Yang X. Excellent antimicrobial properties of mesoporous anatase TiO_2 and Ag/TiO_2 composite films. Microporous Mesoporous Mater. 2008;114(1–3):431–439.

4. Wong MS, Chen CW, Hsieh CC, Hung SC, Sun DS, Chang HH. Antibacterial property of Ag nanoparticle-impregnated N-doped titania films under visible light. Scientific Reports. 2015;5:1–11.

5. Fujishima A, Rao TN, Tryk DA. Titanium dioxide photocatalysis. Journal of Photochemistry and Photobiology C: Photochemistry Reviews. 2000;1(1):1–21.

6. Mills A, Le Hunte S. An overview of semiconductor photocatalysis. Journal of Photochemistry and Photobiology A: Chemistry. 1997;108(1):1–35.

7. Yu B, Leung KM, Guo Q, Lau WM, Yang J. Synthesis of Ag-TiO_2 composite nano thin film for antimicrobial application. Nanotechnology. 2011;22(11):115603 (9pp).

8. Gupta K, Singh RP, Pandey A, Pandey A. Photocatalytic antibacterial performance of TiO_2 and Ag-doped TiO_2 against *S. Aureus. P. Aeruginosa and E. Coli*. Beilstein Journal of Nanotechnology. 2013;4(1):345–351.

9. Akhavan O, Ghaderi E. Self-accumulated Ag nanoparticles on mesoporous TiO_2 thin film with high bactericidal activities. Surface and Coatings Technology. 2010;204(21–22):3676–3683.

10. Shrivastava S, Bera T, Roy A, Singh G, Ramachandrarao P, Dash D. Characterization of enhanced antibacterial effects of novel silver nanoparticles. Nanotechnology. 2007;18(22):103–112.

11. Akkopru B, Anthony A, Mellott NP, Akgun BA, Wren AW, Durucan C, et al. Sol-gel derived silver-incorporated titania thin films on glass: Bactericidal and photocatalytic activity. Journal of Sol-Gel Science Technology. 2011;59(2):228–238.

12. Moellmann J, Ehrlich S, Tonner R, Grimme S. A DFT-D study of structural and energetic properties of TiO_2 modifications. Journal of Physics: Condensed Matter. 2012;24(42):1-5.

13. Wong MS, Sun DS, Chang HH. Bactericidal performance of visible-light responsive titania photocatalyst with silver nanostructures. PLoS One. 2010;5(4):e10394.

14. Petronella F, Truppi A, Ingrosso C, Placido T, Striccoli M, Curri ML, et al. Nanocomposite materials for photocatalytic degradation of pollutants. Catalysis. 2017;281:85–100.

15. Uddin MN, Islam MS, Mazumder MM, Hossain MA, Elias M, Siddiquey IA,

Susan MA, Saha DK, Rahman MM, Asiri AM, Hayami S. Photocatalytic and antibacterial activity of B/N/Ag co-doped CNT–TiO_2 composite films. Journal of Inclusion Phenomena and Macrocyclic Chemistry. 2015 Jun 1;82(1-2):229-234.

16. Hamal DB, Klabunde KJ. Synthesis, characterization, and visible light activity of new nanoparticle photocatalysts based on silver, carbon, and sulfur-doped TiO_2. Journal of Colloid and Interface Scince. 2007;311(2):514–522.

17. Likius DS, Nagai H, Aoyama S, Mochizuki C, Hara H, Baba N, et al. Percolation threshold for electrical resistivity of Ag-nanoparticle/titania composite thin films fabricated using molecular precursor method. Journal of Material Science. 2012;47(8):3890–3899.

18. Tryba B, Piszcz M, Morawski AW. Photocatalytic and Self-Cleaning Properties of Ag-Doped TiO_2. Open Material Science Journal. 2010;4:5–8.

19. Albert E, Albouy PA, Ayral A, Basa P, Csík G, Nagy N, et al. Antibacterial properties of Ag–TiO_2 composite sol–gel coatings. RSC Advances 2015;5(73):59070–59081.

20. Besinis A, Peralta T De, Handy RD, De Peralta T, Handy RD. The antibacterial effects of silver, titanium dioxide and silica dioxide nanoparticles compared to the dental disinfectant chlorhexidine on Streptococcus mutans using a suite of bioassays. Nanotoxicology. 2014;8(1):1–16.

21. Carp O, Huisman CL, Reller A. Photoinduced reactivity of titanium dioxide. Progress Solid State Chemistry. 2004;32(1–2):33–177.

22. Pelaez M, Nolan NT, Pillai SC, Seery MK, Falaras P, Kontos AG, et al. A

review on the visible light active titanium dioxide photocatalysts for environmental applications. Applied Catalysis B: Environmental. 2012;125:331–349.

23. Petica A, Florea A, Gaidau C, Balan D, Anicai L. Synthesis and characterization of silver-titania nanocomposites prepared by electrochemical method with enhanced photocatalytic characteristics, antifungal and antimicrobial activity. Journal of Materials Research and Technology. 2017;6(4):1–13.

24. Zhou R, Lin S, Zong H, Huang T, Li F, Pan J. Continuous Synthesis of Ag/TiO_2 Nanoparticles with Enhanced Photocatalytic Activity by Pulsed Laser Ablation. Journal of Nanomaterials. 2017;(24):4-9.

25. Damodar RA, You SJ, Chou HH. Study the self cleaning, antibacterial and photocatalytic properties of TiO_2 entrapped PVDF membranes. Journal of Hazardous Materials. 2009;172(2–3):1321–1328.

26. Sun D-S, Kau J-H, Huang H-H, Tseng Y-H, Wu W-S, Chang H-H. Antibacterial Properties of Visible-Light-Responsive Carbon-Containing Titanium Dioxide Photocatalytic Nanoparticles against Anthrax. Nanomaterials. 2016;6(12):237–249.

27. Fujishima A, Honda K. Electrochemical Photolysis of Water at a Semiconductor Electrode. Nature. 1972;238(5358):37–38.

28. Hashimoto K, Irie H, Fujishima A. TiO_2 Photocatalysis: A Historical Overview and Future Prospects. Japanese Journal of Applied Physics. 2005;44(12):8269–8285.

29. Shon H.K, Phuntsho S., Okour Y., Cho D.L., Kim J.B., Na S. KJH. Visible

responsive titanium dioxide (TiO_2). A Review. Journal of the Korean Industry and Engeering. 2007;19(1):1–29.

30. Frank SN, Bard AJ. Heterogeneous photocatalytic oxidation of cyanide and sulfite in aqueous solutions at semiconductor powders. Journal of Physical Chemistry. 1998;81(15):1484–1488.

31. Alfonso V. Developments in solar photocatalysis for water purification. Chemosphere. 36(12):2593–2606.

32. O'Regan B, Gratzel M. A Low-Cost, High-Efficiency Solar-Cell Based on Dye-Sensitized Colloidal TiO_2 Films. Nature. 1991;353(6346):737–740.

33. Zou X, Silva R, Huang X, Al-Sharab JF, Asefa T. A self-cleaning porous TiO_2–Ag core–shell nanocomposite material for surface-enhanced Raman scattering. Chemical Communications. 2013;49(4):382–384.

34. Wu TS, Wang KX, Li GD, Sun SY, Sun J, Chen JS. Montmorillonite-Supported Ag/TiO2nanoparticles: An efficient visible-Light bacteria photodegradation material. ACS Applied Materials Interfaces. 2010;2(2):544–550.

35. Nosaka Y, Matsushita M, Nishino J, Nosaka A, Nosaka Y, Matsushita M, et al. Nitrogen-doped titanium dioxide photocatalysts for visible response prepared by using organic compounds Nitrogen-doped titanium dioxide photocatalysts for visible response prepared by using organic compounds. Science and Technology of Advanced Materials. 2005;6(2):143-148.

36. Yates HM, Nolan MG, Sheel DW, Pemble ME. The role of nitrogen doping on the development of visible light-induced photocatalytic activity in thin TiO_2 films grown on glass by chemical vapour deposition. Journal of Photochemistry

and Photobiology A: Chemistry. 2006;179(1–2):213–223.

37. Zhang FJ, Oh WC. Characterization and photonic effect of novel Ag-CNT/TiO_2 composites and their bactericidal activities. Bulletin of Korean Chemical Society. 2010;31(7):1981–1987.

38. Morales-torres S, Pastrana-martínez LM. Design of graphene-based TiO_2 photocatalysts — A Review. Environmental Science and Pollution Research. 2012;3676–3687.

39. Curnan MT, Kitchin JR. Investigating the energetic ordering of stable and metastable TiO_2 polymorphs using DFT+ U and hybrid functionals. The Journal of Physical Chemistry C. 2015;119(36):21060-21071.

40. Cheng H, Ma J, Zhao Z, Qi L. Hydrothermal Preparation of Uniform Nanosize Rutile and Anatase Particles. Chemistry of Materials. 1995;7(4):663–671.

41. Hoffmann MR, Martin ST, Choi W, Bahnemann DW. Environmental Applications of Semiconductor Photocatalysis. Chemical Reviews. 1995;95(1):69–96.

42. Keidel E. The effect on the light fastness of coal tar dye paints by titanium white. Farben-Zeitung. 1929;34:1242–1243.

43. Serpone N, Emeline A V., Horikoshi S, Kuznetsov VN, Ryabchuk VK. On the genesis of heterogeneous photocatalysis: A brief historical perspective in the period 1910 to the mid-1980s. Photochemical & Photobiological Sciences. 2012;11(7):1121-1150.

44. Sunada K, Watanabe T, Hashimoto K. Bactericidal activity of copper-deposited

TiO_2 thin film under weak UV light illumination. Environmental Science & Technology. 2003;37(20):4785-4789.

45. Guo S, Wu Z, Zhao W. TiO_2-based building materials: Above and beyond traditional applications. Chinese Science Bulletin. 2009;54(7):1137–1142.

46. Kikuchi Y, Sunada K, Iyoda T, Hashimoto K, Fujishima A. Photocatalytic bactericidal effect of TiO2 thin films: dynamic view of the active oxygen species responsible for the effect. Journal of Photochemistry and Photobiology A: Chemistry.1997;106(1–3):51–56.

47. Sunada K, Kikuchi Y, Hashimoto K, Fujishima A. Bactericidal and Detoxification Effects of TiO_2 Thin Film Photocatalysts. Environmental Science & Technology. 1998;32(5):726–728.

48. Minabe T, Tryk DA, Sawunyama P, Kikuchi Y, Hashimoto K, Fujishima A. TiO_2-mediated photodegradation of liquid and solid organic compounds. Journal of Photochemistry and Photobiology A: Chemistry . 2000;137(1):53–62.

49. Zaleska A. Doped-TiO_2 : A Review. Recent Patents on Engeering. 2008;2(1):157–164.

50. Cai R, Hashimoto K, Itoh K, Kubota Y, Fujishima A. Photokilling of Malignant-Cells with Ultrafine TiO_2 Powder. Bulletin of the Chemical Society of Japan. 1991;64(4):1268–1273.

51. Cai R, Hashimoto K, Kubota Y, Fujishima A. Increment of Photocatalytic Killing of Cancer Cells Using TiO_2 with the Aid of Superoxide Dismutase. Chemitry Letters . 1992;21(3):427–430.

52. Cai R, Kubota Y, Shuin T, Sakai H, Hashimoto K, Fujishima A. Induction of Cytotoxicity by Photoexcited TiO_2 Particles. Cancer Research. 1992;52(4):2346–2348.

53. Sato S. Photocatalytic activity of NOx-doped TiO_2 in the visible light region. Chemical Physics Letters. 1986;123(1–2):126–128.

54. Sato S, Nakamura R, Abe S. Visible-light sensitization of TiO_2 photocatalysts by wet-method N doping. Applied Catalysis A: General. 2005;284(1–2):131–137.

55. Xie Y, Li Y, Zhao X. Low-temperature preparation and visible-light-induced catalytic activity of anatase F–N-codoped TiO_2. Journal of Molecular Catalysis A: Chemical. 2007;277(1–2):119–126.

56. Liu S, Yu J, Wang W. Effects of annealing on the microstructures and photoactivity of fluorinated N-doped TiO_2. Physical Chemistry Chemical Physics. 2010;12(38):12308-12315.

57. Asahi R, Morikawa T, Ohwaki T, Aoki K, Taga Y. Visible-light photocatalysis in nitrogen-doped titanium oxides. Science. 2001;293(5528):269–271.

58. Asahi AR, Morikawa T, Ohwaki T, Aoki K, Taga Y, Lee V, et al. Visible-Light Photocatalysis in Nitrogen-Doped Titanium Oxides Published by : American Association for the Advancement of Science Linked references are available on JSTOR for this article : Visible-Light Visible-Light Photocatalysis Photocatalysis in N. 2017;293(5528):269–271.

59. Ihara T, Miyoshi M, Iriyama Y, Matsumoto O, Sugihara S. Visible-light-active titanium oxide photocatalyst realized by an oxygen-deficient structure and by

nitrogen doping. Applied Catalysis B: Environmental. 2003;42(4):403–409.

60. Irie H, Washizuka S, Yoshino N, Hashimoto K. Visible-light induced hydrophilicity on nitrogen-substituted titanium dioxide films. Chemical Communications. 2003(11):1298-1299.

61. Nagai H, Mochizuki C, Hara H, Takano I, Sato M. Enhanced UV-sensitivity of vis-responsive anatase thin films fabricated by using precursor solutions involving Ti complexes. Sol Energy Mater Sol Cells. 2008;92(9):1136–1144.

62. Wang L, Ali J, Zhang C, Mailhot G, Pan G. Simultaneously enhanced photocatalytic and antibacterial activities of TiO_2/Ag composite nanofibers for wastewater purification. Journal of Environmental Chemical Engeering. 2017;5(6):5293-6216.

63. Choi W, Termin A, Hoffmann MR. The Role of Metal Ion Dopants in Quantum-Sized TiO_2: Correlation between Photoreactivity and Charge Carrier Recombination Dynamics. Journal of Physical Chemistry. 1994;98(51):13669–13679.

64. Kang M. The superhydrophilicity of Al–TiO_2 nanometer sized material synthesized using a solvothermal method. Materials Letters. 2005;59(24–25):3122–3127.

65. Li FB, Li XZ. The enhancement of photodegradation efficiency using Pt–TiO_2 catalyst. Chemosphere. 2002;48(10):1103–1111.

66. Demeestere K, Dewulf J, Ohno T, Salgado PH, Van Langenhove H. Visible light mediated photocatalytic degradation of gaseous trichloroethylene and dimethyl sulfide on modified titanium dioxide. Applied Catalysis B:

Environmental. 2005;61(1–2):140–149.

67. Dvoranová D, Brezová V, Mazúr M, Malati MA. Investigations of metal-doped titanium dioxide photocatalysts. Applied Catalysis B: Environmental. 2002;37(2):91–105.

68. Fuerte A, Hernández-Alonso MD, Maira AJ, Martínez-Arias A, Fernández-García M, Conesa JC, et al. Visible light-activated nanosized doped-TiO_2 photocatalysts. Chemical Communications. 2001(24):2718–2719.

69. Wu JC-S, Chen C-H. A visible-light response vanadium-doped titania nanocatalyst by sol–gel method. Journal of Photochemistry and Photobiology A: Chemistry. 2004;163(3):509–515.

70. Yamashita H, Harada M, Misaka J, Takeuchi M, Ikeue K, Anpo M. Degradation of propanol diluted in water under visible light irradiation using metal ion-implanted titanium dioxide photocatalysts. Journal of Photochemistry and Photobiology A: Chemistry. 2002;148(1–3):257–261.

71. Behar D, Rabani J. Kinetics of hydrogen production upon reduction of aqueous TiO_2 nanoparticles catalyzed by Pd0, Pt0, or Au0 coatings and an unusual hydrogen abstraction; steady state and pulse radiolysis study. The Journal of Physical Chemistry B. 2006;110(17):8750-8755.

72. Zeng Y, Wu W, Lee S, Gao J. Photocatalytic performance of plasma sprayed Pt-modified TiO_2 coatings under visible light irradiation. Catalysis Communications. 2007;8(6):906–912.

73. Wang W, Zhang J, Chen F, He D, Anpo M. Preparation and photocatalytic properties of Fe^{3+}-doped Ag@TiO_2 core–shell nanoparticles. Journal of Colloid

and Interface Science. 2008;323(1):182–186.

74. You X, Chen F, Zhang J, Anpo M. A novel deposition precipitation method for preparation of Ag-loaded titanium dioxide. Catalysis Letters .2005;102(3–4):247–250.

75. Sharma VK, Yngard RA, Lin Y. Silver nanoparticles: Green synthesis and their antimicrobial activities. Advances in Colloid and Interface Science. 2009;145(1–2):83–96.

76. Seery MK, George R, Floris P, Pillai SC. Silver doped titanium dioxide nanomaterials for enhanced visible light photocatalysis. Journal of Photochemistry and Photobiology A: Chemistry. 2007;189(2–3):258–263.

77. Nolan NT, Seery MK, Hinder SJ, Healy LF, Pillai SC. A Systematic Study of the Effect of Silver on the Chelation of Formic Acid to a Titanium Precursor and the Resulting Effect on the Anatase to Rutile Transformation of TiO_2. The Journal of Physical Chemistry C. 2010;114(30):13026–13034.

78. Ouyang J, Chang M, Li X. CdS-sensitized ZnO nanorod arrays coated with TiO_2 layer for visible light photoelectrocatalysis. Journal of Materials Science. 2012;47(9):4187–4193.

79. Wu T, Lin T, Zhao J, Hidaka H, Serpone N. TiO_2-assisted photodegradation of dyes. 9. Photooxidation of a squarylium cyanine dye in aqueous dispersions under visible light irradiation. Environmental Science & Technology. 1999;33(9):1379-1387.

80. Xu Y, Langford CH. UV-or visible-light-induced degradation of X_3B on TiO_2 nanoparticles: The influence of Adsorption. Langmuir. 2001;17(3):897-902.

81. Ahmed R, Will G, Bell J, Wang H. Size-dependent photodegradation of CdS particles deposited onto TiO_2 mesoporous films by SILAR method. Journal of Nanoparticle Research. 2012;14(9):1–13.

82. Soga T, editor. Nanostructured Materials for Solar Energy Conversion. 1st ed. Nagoya: Elsevier; 2006. 615.

83. Espinosa A, Curcio A, Cabana S, Radtke G, Bugnet M, Kolosnjaj-Tabi J, Péchoux C, Alvarez-Lorenzo C, Botton GA, Silva AK, Abou-Hassan A. Intracellular Biodegradation of Ag Nanoparticles, Storage in Ferritin, and Protection by a Au Shell for Enhanced Photothermal Therapy. ACS nano. 2018;12(7):6523-6535.

84. Padeletti G, Fermo P. How the masters in Umbria, Italy, generated and used nanoparticles in art fabrication during the renaissance period. Applied Physics A. Materials Science & Processing. 2003;76(4):515–525.

85. Zhang Q, Uchaker E, Candelaria SL, Cao G. Nanomaterials for energy conversion and storage. Chemical Society Reviews. 2013;42(7):3127-3171.

86. Iwakura I, Yabushita A, Kobayashi T. Why is Indigo Photostable over Extremely Long Periods?. Chemistry Letters. 2009;38(11):1020–1021.

87. Caroscio M. Archaeological Data and Written Sources: Lustreware Production in Renaissance Italy, a Case Study. European Journal of Archaeology. 2010;13(2):217–244.

88. Mattei, Pietro ; Cecchetti T, editors. Mastro Giorgio : l'uomo, l'artista, l'imprenditore. Perugia: OpenBibArt. Camera di Commercio Industria Artigianato e Agricoltura. 1995:239.

89. Turkevich J, Stevenson PC, Hillier J. A study of the nucleation and growth processes in the synthesis of colloidal gold. Discussions of the Faraday Society. 1951;11:55-75.

90. Lee C, Meisel D, Lee PC, Meisel D. Adsorption and surface-enhanced Raman of dyes on silver and gold sols. The Journal of Physical Chemistry. 1982;86(17):3391–3395.

91. Iravani S, Korbekandi H, Mirmohammadi SV, Zolfaghari B. Synthesis of silver nanoparticles: chemical, physical and biological methods. Research in Pharmaceutical Sciences. 2014;9(6):385-406.

92. Park HH, Zhang X, Choi YJ, Kim H, Park HH, Hill RH. Facile synthesis and size control of Ag nanoparticles by a photochemical reduction at room temperature. Journal of the Ceramic Society of Japan. 2010;118(1383):1002-1005.

93. Horvth IT, Anastas PT. Innovations and green chemistry. Chemical Reviews. 2007;107:2169-3173.

94. Kuntyi O, Okhremchuk Y, Bilan' O, Hapke J, Saldan I. Silver particles growth by pulse electrolysis in acetonitrile solutions. Central European Journal of Chemistry. 2013;11(4):514–518.

95. V. Dorozhkin S. Nanodimensional and Nanocrystalline Calcium Orthophosphates. Journal of Biomedical Engeering. 2012;2(3):48–97.

96. Creighton JA, Blatchford CG, Albrecht MG. Plasma resonance enhancement of Raman scattering by pyridine adsorbed on silver or gold sol particles of size comparable to the excitation wavelength. Journal of the Chemical Society,

Faraday Transactions 2: Molecular and Chemical Physics. 1979;75:790-798.

97. Pastoriza-Santos I, Liz-Marzán LM. Formation and stabilization of silver nanoparticles through reduction by N, N-dimethylformamide. Langmuir. 199;15(4):948-951.

98. Almeida E, Moreira ACL, Brito-Silva AM, Galembeck A, De Melo CP, De L, et al. Ultrafast dephasing of localized surface plasmons in colloidal silver nanoparticles: The influence of stabilizing agents. Applied Physics B: Lasers Opt. 2012;108(1):9–16.

99. Lungu M, Gavriliu Ş, Enescu E, Ion I, Brătulescu A, Mihăescu G, Măruţescu L, Chifiriuc MC. Silver–titanium dioxide nanocomposites as effective antimicrobial and antibiofilm agents. Journal of Nanoparticle Research. 2014;16(1):2203-2218.

100. Dinh CT, Nguyen TD, Kleitz F, Do TO. A new route to size and population control of silver clusters on colloidal TiO_2 nanocrystals. ACS Applied Materials & Interfaces. 2011;3(7):2228-2234.

101. Rifai S, Breen CA, Solis DJ, Swager TM. Facile in situ silver nanoparticle formation in insulating porous polymer matrices. Chemistry of Materials. 2006;18(1):21-25.

102. Nagai H., Sato M. Heat Treatment in Molecular Precursor Method for Fabricating Metal Oxide Thin Films. In: Czerwinski F., editor. Heat Treatment – Conventional and Novel Applications. Rijeka:InTech; 2012. pp. 103–124.

103. Banerjee AN. The design, fabrication, and photocatalytic utility of nanostructured semiconductors: Focus on TiO_2-based nanostructures.

Nanotechnology, Science and Applications. 2011;4(1):35–65.

104. Campbell SA, Kim HS, Gilmer DC, He B, Ma T, Gladfelter WL. Titanium dioxide (TiO_2)-based gate insulators. IBM Journal of Research and Development. 1999;43(3):383-392.

105. Wang Z, Helmersson U, Käll PO. Optical properties of anatase TiO_2 thin films prepared by aqueous sol–gel process at low temperature. Thin Solid Films. 2002;405(1-2):50-54.

106. Sakka S. The current state of sol-gel technology. Journal of Sol-Gel Science and Technology. 1994;3(2):69-81.

107. Sakka S. Gel method for making glass. Treatise on Materials Science and Technology. 1982;22:129-167.

108. Mazdiyasni, Dolloff RT, Smith JS. Preparation of High- Purity Submicron Barium Titanate Powders. Journal of the American Ceramic Society. 1969;52(10):523-526.

109. Sakka S, Kamiya K. The sol-gel transition in the hydrolysis of metal alkoxides in relation to the formation of glass fibers and films. Journal of Non-Crystalline Solids. 1982;48(1):31-46.

110. Hu L, Yoko T, Kozuka H, Sakka S. Effects of solvent on properties of sol—gel-derived TiO_2 coating films. Thin solid films. 1992;219(1-2):18-23.

111. Dimitriev Y, Ivanova Y, Iordanova R. History of sol-gel science and technology. Journal of the University of Chemical Technology and Metallurgy. 2008;43(2):181-192.

112. Tseng TK, Lin YS, Chen YJ, Chu H. A review of photocatalysts prepared by sol-gel method for VOCs removal. International Journal of Molecular Science. 2010;11(6):2336–2361.

113. Chilibon I, Marat-Mendes JN. Ferroelectric ceramics by sol–gel methods and applications: a review. Journal of Sol-gel Science and Technology. 2012;64(3):571-611.

114. Chen X, Mao SS. Titanium dioxide nanomaterials: synthesis, properties, modifications, and applications. Chemical Reviews. 2007;107(7):2891-2959.

115. Sato M, Hara H, Nishide T, Sawada Y. A water-resistant precursor in a wet process for TiO_2 thin film formation. Journal of Materials Chemistry. 1996;6(11):1767-1770.

116. Nishide T, Sato M, Hara H. Crystal structure and optical property of TiO_2 gels and films prepared from Ti-edta complexes as titania precursors. Journal of Materials Science. 2000;35(2):465-469.

117. Sato M, Hara H, Kuritani H, Nishide T. Novel route to Co_3O_4 thin films on glass substrates via N-alkyl substituted amine salt of Co (III)-EDTA complex. Solar Energy Materials and Solar Cells. 1997;45(1):43-49.

118. Sato M, Tanji T, Hara H, Nishide T, Sakashita Y. $SrTiO_3$ film fabrication and powder synthesis from a non-polymerized precursor system of a stable Ti(IV) complex and Sr(II) salt of edta. Journal of Materials Chemistry. 1999;9(7):1539-1542.

119. Nagai H, Hasegawa M, Hara H, Mochizuki C, Takano I, Sato M. An important factor for controlling the photoreactivity of titania: O-deficiency of anatase thin

films. Journal of Materials Science. 2008;43(21):6902-6911.

120. Nagai H, Aoyama S, Hara H, Mochizuki C, Takano I, Honda T, Sato M. Photoluminescence and photoreactivity affected by oxygen defects in crystal-oriented rutile thin film fabricated by molecular precursor method. Journal of Materials Science. 2010;45(20):5704-5710.

121. Mochizuki C, Sasaki Y, Hara H, Sato M, Hayakawa T, Yang F, Hu X, Shen H, Wang S. Crystallinity control of apatite through Ca- EDTA complexes and porous composites with PLGA. Journal of Biomedical Materials Research Part B: Applied Biomaterials. 2009;90(1):290-301.

122. Honda T, Oda T, Mashiyama Y, Hara H, Sato M. Fabrication of c- axis oriented Ga- doped MgZnO- based UV transparent electrodes by molecular precursor method. Physica Status Solidi C. 2010;7(10):2471-2473.

123. Christopher P, Xin H, Linic S. Visible-light-enhanced catalytic oxidation reactions on plasmonic silver nanostructures. Nature Chemistry. 2011;3(6):467–472.

124. Hou W, Hung WH, Pavaskar P, Goeppert A, Aykol M, Cronin SB. Photocatalytic conversion of CO_2 to hydrocarbon fuels via plasmon-enhanced absorption and metallic interband transitions. Acs Catalysis. 2011;1(8):929-936.

125. Reidy B, Haase A, Luch A, Dawson K, Lynch I. Mechanisms of silver nanoparticle release, transformation and toxicity: A critical review of current knowledge and recommendations for future studies and applications. Materials. 2013;6(6):2295-2350.

126. Siderov V, Mladenova D, Yordanov R, Milenkov V, Ohlidal M, Salyk O, Zhivkov I, Weiter M. Film thickness measurement by optical profilometer MicroProf FRT. Bulgarian Chemical Communications. 2013;45:194-197.

127. Lalitha MK. Manual on antimicrobial susceptibility testing. Performance standards for antimicrobial testing: Indian Journal of Medical Research. 88(2008):455-460.

128. Holzwarth U, Gibson N. The Scherrer equation versus the "Debye-Scherrer equation." Nature Nanotechnol. 2011;6(9):534–534.

129. Rochholz H, Bocchio N, Kreiter M. Tuning resonances on crescent-shaped noble-metal nanoparticles. New Journal of Physics. 2007;9(3):53-56.

130. Ochoo L, Migwi C, Okumu J. Damping effect of the inner band electrons on the optical absorption and bandwidth of metal nanoparticles. Journal of Nanoparticle Research. 2012;14(12):1261-1262.

131. Subash B, Krishnakumar B, Velmurugan R, Swaminathan M. Photodegradation of an azo dye with reusable SrF_2–TiO_2 under UV light and influence of operational parameters. Separation and Purification Technology. 2012;101:98-106.

132. Panáček A, Kvitek L, Prucek R, Kolář M, Večeřová R, Pizúrová N, Sharma VK, Nevěčná TJ, Zbořil R. Silver colloid nanoparticles: synthesis, characterization, and their antibacterial activity. The Journal of Physical Chemistry B. 2006;110(33):16248-16253.

133. Kim JY, Lee C, Cho M, Yoon J. Enhanced inactivation of *E. coli* and MS-2 phage by silver ions combined with UV-A and visible light irradiation. Water Research. 2008;42(1-2):356-362.

APPENDIX

Appendix I: Materials used in this study

Table 1: Chemicals used to prepare precursor solutions.

Chemical name	**Chemical formula**	**Amount used (g) per trial**	**Moles (mmol)**
Dibutylamine	$C_8H_{19}N$	3.58[a], 0.56[b]	27.7[a], 4.3[b]
Ethylenediamine-N,N,N',N'-tetraacetic acid	$C_{10}H_{16}N_2O_8$	3.56[a]	12.2[a]
Ethanol (99.9%)	C_2H_5OH	10[a], 1.0[b]	217[a], 21.7[b]
Methanol	CH_3OH	10[a]	312[a]
Silver Acetate	CH_3COOAg	0.24[b]	1.4[b]
Titanium tetraisopropoxide	$Ti(O^iPr)_4$	3.47[a]	12.2[a]
Hydrogen peroxide	H_2O_2	1.56[a]	13.8[a]

[a]*Amount used to prepare the Titania precursor solution.*

[b]*Amount used to prepare the silver precursor solution.*

Table 2: Consumables used in the antibacterial susceptibility test.

Identity of consumable	**Amount**
Nutrient Agar	-
Nutrient broth	-
E-coli ATCC25922	-
Barium chloride ($BaCl_2$)	0.048M
Sulphuric acid (H_2SO_4)	0.18M
Gentamicin	50µg/ml

Appendix II: Data for mean film thickness

Table 3: Mean film thickness for selected films.

Representative sample	Mean film thickness (nm)
20 mol% Ag	**100 (0.5)**
40 mol% Ag	**100**
60 mol% Ag	**100**
80 mol% Ag	**260 (1)**
Bare TiO_2	**130 (3)**

**Three successive measurements were taken per concentration.*
**Estimated standard deviations are presented in parentheses.*

Appendix III: Raw data for the disk diffusion method

Table 4: Experimental results for the antibacterial activity evaluation of thin films.

Film	Exp. 1	Exp. 2	Exp. 3	Mean inhibition zone	STDEV	SE
Pure TiO_2	0.0	0.0	0.0	0.0	0.00	0
Pure Ag	0.0	0.0	0.0	0.0	0.00	0.
10 mol% Ag	11	11.5	11	11.2	0.29	0.09129
20 mol% Ag	12.5	12	12	12.2	0.29	0.09129
30 mol% Ag	12	13	13.5	12.8	0.76	0.24152
40 mol% Ag	13.5	13.5	14	13.7	0.29	0.09129
50 mol% Ag	14.5	15	14.5	14.7	0.29	0.09129
60 mol% Ag	15.5	15	15.5	15.3	0.29	0.09129
70 mol% Ag	19	18.5	19	18.8	0.29	0.09129
80 mol% Ag	15.5	15.5	15.5	15.5	0.00	0
90 mol% Ag	15	15.5	15	15.2	0.29	0.09129
Gentamicin	15.5	14.5	15.5	15.2	0.58	0.18257

Appendix IV; Raw data for the viable cell count method

Table 5: In the dark

Film	Exp. 1 (cfu)	Exp.2 (cfu)	Exp. 3 (cfu)	Mean cfu	cfu (- control)	Colony inhibited	% Inhibition	STDEVS
Gentamicin	0	0	0	0	296	296	100.0	0.0
Bare glass	296	298	294	296	296	0	0.0	2.0
Pure TiO_2	291	294	296	293.6667	296	2	0.8	2.5
PureAg	282	281	284	282.3333	296	14	4.6	1.5
20 mol% Ag	271	274	269	271.3333	296	25	8.3	2.5
30 mol% Ag	268	267	270	268.3333	296	28	9.3	1.5
40 mol% Ag	263	261	263	262.3333	296	34	11.4	1.2
50 mol% Ag	259	258	254	257	296	39	13.2	2.6
60 mol% Ag	255	252	257	254.6667	296	41	14.0	2.5
70 mol% Ag	250	253	251	251.3333	296	45	15.1	1.5
80 mol% Ag	247	248	243	246	296	50	16.9	2.6
90 mol% Ag	241	245	242	242.6667	296	53	18.0	2.1

Table 6: Under visible light

Films	Exp. 1	Exp. 2	Exp. 3	Mean cfu	Mean CFU (-control)	Colony Inihibited	% Inhibition	STDEVS
Getamicin	0	0	0	0	287	287	100	0
Bare glass	287	273	284	281	287	6	2	7.3711148
Pure TiO_2	279	274	278	277	287	10	3	2.6457513
Pure Ag	263	268	273	268	287	19	7	5
20 mol% Ag	248	254	251	251	287	36	13	3
30 mol% Ag	214	211	198	208	287	79	28	8.5049005
40 mol% Ag	205	206	199	203	287	84	29	3.7859389
50 mol% Ag	104	97	96	99	287	188	66	4.3588989
60 mol% Ag	79	68	78	75	287	212	74	6.0827625
70 mol% Ag	32	41	38	37	287	250	87	4.5825757
80 mol% Ag	46	53	59	53	287	234	82	6.5064071
90 mol% Ag	52	56	58	55	287	232	81	3.0550505